Dear Editors of Atmospheric Chemistry and Physics,

On behalf of the co-authors (Liu, Ishizuka, Mikami and Shao), I wish to thank the two referees for their very helpful comments and also two readers who send us their comments. These comments are now considered in the revised version of the paper for your consideration. The point by point reply and the revised manuscript are uploaded.

Please address all correspondence to:

Prof. Yaping Shao
Institute for Geophysics and Meteorology, University of Cologne, Germany
Tel: + 49 (0) 221 470-3688
Fax: + 49 (0) 221 470-5161
E-mail: yshao@uni-koeln.de (preferred contact address)

Reply to SC2:

We wish to thank SC2 for her efforts to work through our paper and providing very helpful comments. Our reply to her comments are as follows:

Comment to Fig 3: thanks for this very good suggestion. We will slightly change the graph to make the hysteresis clearer

Comment to Fig 4: As suggested, we will modify the figure

L247: Accepted

L268-269: Yes. This can be seen from size solved *Q* data

L378-387: Thanks to SC2 for this comment, in which she stated that "*I think making this conclusion here is somewhat problematic, because it is based on data sampled for Q < 3 g/m/s. Although Q depends on u* and therefore small Q are likely to coincide with small u*, u* might not be the only reason for Q to be small. Therefore, sampling for small Q might introduce a bias by selecting only those Q that already tend to have small c0, in particular around 3 g/m/s, the selected cut-off. The result of smaller c0 for smaller fluxes can therefore in my opinion not unambiguously be used to prove a dependence of c0 on u*/turbulence*."

This discussion motivated us to think deeper about the process of saltation and we would like to retain our argument in the text. Basically, weak saltation occurs in case of smaller friction velocity. We now know that for smaller friction velocity, saltation becomes gradually more intermittent. Therefore, c0, a description of the relation between time averaged saltation flux and time averaged friction velocity becomes smaller. We added a sentence and hope it becomes clearer.

L410-412: Clarified.

General comments: SC2 made two general comments as follows: "I have two general comments/questions:
(1) I wonder whether there might be a (small) temporal delay between measured winds and the associated measured Q_1s which could depend on particle size (due to the particles' inertia) and which might have an effect on the parameter results. Perhaps this could be worth exploring, even if only to rule

it out. Due to the necessary temporal integration of u_*, this is likely invisible though (if present at all). (2) How do you think the parameter PDFs would change for a different (perhaps less ideal) surface? I think that a brief discussion on that would be very interesting."

Due to data limitation, we do not have shear stress data with one second resolution. Consequently, we were unable to check the correlation of shear stress and sand drift at frequency of 1 Hz. The question rated by SC2 is certainly important, which we will investigate with better experiment design and instrumentation. Our data show that the two quantities are well correlated at the frequencies of large eddies and synoptic events, a pronounced phase shift between the two quantities is so far not identified. Earlier studies (e.g. Butterfield, 1991) suggest that the response time of the aeolian surface is about 1 second, therefore, we do not think there are phase differences between saltation flux and shear stress on time scales over one minute or longer.

We thank SC2 for this comment. We will add a paragraph of our view on the problem. We will also cite two recent papers by Raffaele et al. (2016; 2018). The added paragraph will be as follows:

In this study, we highlighted the need to better understand parameter uncertainty in saltation models and the processes responsible for the uncertainty. The concept of threshold friction velocity as a stochastic variable was first proposed in Shao (2001). Raffaele et al. (2016) more systematically examined the probabilistic distribution of u_{*t} using data compiled from earlier publications. Raffaele et al. (2018) then studied how u_{*t} uncertainties propagate in saltation flux calculations and reported that in the case of small excess shear stress, all models they tested amplify the uncertainty in estimated saltation flux, especially for coarse sand. This finding is consistent with our notion that c_0 also is a stochastic variable. Our estimate of the parameter uncertainties is based on the data of a relatively simple aeolian surface. For more complex surfaces, we expect the parameter uncertainties to be even more pronounced.

RC1: We wish to thank Dr. Gilles for his efforts for working through our draft and providing very helpful comments and very detailed editorial suggestions. Most of his editorial suggestions are accepted, as reflected in the revised manuscript. Our reply to his other comments are as follows:

L44: We kept our original formulation to stress that variations in threshold can also lead to intermittent saltation.

We accepted all his editorial comments and answered all his queries. In particular, we did more work to Fig. 11.

RC2: We are grateful to RC2 for his/her constructive comments. We feel encouraged that RC2 finds our work "of great interest" and we find his/her critical comments accurate and very helpful. In the revised manuscript, we have tried to accommodate these comments. Our point by point reply is as follows:

Major comments:

Introduction: The introduction clearly state the position of the problem. Some suggestions to better organize the text are given in "Minor comments".

We modified the text according to the minor suggestions.

Part2: I would suggest to separate by subtitled the first part describing the computation method and the one describing the data and their pre-treatment. In fact the reading could be more easy if the data were described first and the computing method after.

A few lines to introduce the objective of the part concerning the computing algorithm and to make the link with the introduction are absolutely required. Several method are briefly described to end up with the one selected by the authors without arguing why this method is better adapted than the others to analyse saltation and wind friction velocities datasets.

At the end of the chapter (page4 line 141) the reader does not really know what is computed with this method regarding to the different results presented in the following parts.

We thank the referee for the comments. We have substantially reworked on the section and hope the description is now clearer.

Online163-164, the author mention that the fitting of the vertical profile lead to inaccuracies in the estimation of Q, but that it would not affect the results of this study. A quantitative estimation of these accuracies is needed.

The request of the referee is understood, but unfortunately, we are not able to give a more detailed statement on the absolute accuracy of the Q measurements using the SPCs. Care was taken such that individual SPC works properly (e.g. wind-tunnel calibration), but as measurements were only made at 3 levels, the profile of saltation flux density was under represented. However, as our study is mainly on temporal variations of saltation fluxes, the inaccuracy in the absolute values should not significantly alter our conclusions. We slightly modified the text.

The authors used a data set of U* average over one minute. A discussion on the relevance of this time-scale would be welcome. U* is more commonly averaged over tens of minutes to represent the average effect of the main turbulent structures.

This is a challenging question, as there is really no standard for how long one should average wind to "correctly" estimate u_*, but we can answer the question from three perspectives. First, if u* is used as a scaling velocity for turbulence properties in atmospheric boundary layer, e.g., turbulence intensity, eddy diffusivity, M-O similarity functions etc., it seems necessary to average over sufficiently long time to obtain a more or less "constant" shear stress and u_*. Second, if u* is merely a surrogate for shear stress and one is interested in the variations of the shear stress, then shorter averaging times are justified, subject to the condition that the response of aeolian fluxes to shear stress is faster. We know (roughly) from earlier studies (Butterfield, 1991; Anderson and Haff, 1988) that the response time of aeolian fluxes

in turbulent flows is of the order of one second. Third, to derive meaningful shear stress from wind profile, what averaging wind data do we have to use? This depends on whether the assumptions of flow steady state and horizontal homogeneity are satisfied. The JADE site is a flat farm land, such that the use of wind profile data for deriving shear stress for 1-minute intervals can be justified. We added a paragraph to this effect in the revised manuscript.

Part3: This part should be divided in subsections (time series and wind dependence of Q; Pdf; intermittency; power spectra). In general, the figures and interpretations given in part 3 are not sufficiently described and commented to be fully understood and appreciate.

We went through the text and tried to add clarifications.

a) Time series: Figures 1 and 2 shows times series of Q and U*, with a 12-days data set and a zoom on a two days data sets that is not included in the previous 12 Interactive days period. These figures (b) are not commented in the text and at this stage of the manuscript, the reader cannot understand why they are shown.

We reformulated the section and made changes to the graphs. The purpose of this section is to show the time series this study is based on and discuss some turbulent features which we can identify directly by looking at the times series.

Page 13, line 203-213: the behavior of Q is very different on day 71 and72 and the authors argued that the hysteresis behavior during these two days can be due to changes in surface properties and atmospheric turbulence. Is there any observational evidences for these differences or is it just speculative? If the atmospheric turbulence is different, one may expect different results for these two specifics days in the following parts of the paper. But they are no more evoked in the following.

There is some evidence for this. We substantially changed the text and added Fig. 3d to Fig. 3 showing the time series of ($u_{*1min} - u_{*30min}$) as a measure of turbulent fluctuations. It is seen that saltation is usually not only associated with high surface shear stress but also with high shear stress fluctuations. The profound difference in the $Q \sim u_*$ relationship between D70-71 and D72 (Fig. 3b) can be attributed to the strong differences in turbulent fluctuations between them: D70-71 was a hot and gusty day with top (2 cm) soil temperature reaching 53^{o}C, while D72 was a cooler and less gusty day with soil temperature about 5^{o}C lower. It seems that saltation hysteresis cannot be simply attributed to turbulence. We speculate that it is more likely to be related to flow-saltation feedbacks (e.g. stronger splash entrainment in the strengthening phase) and the modification of surface aerodynamic conditions (e.g. particle sorting and reduced surface roughness Reynolds number). But we need an extra study to fully answer the question.

b) Probability density functions: Figure4 present the probability density function of the saltation fluxes for different particles sizes. How does the pdf of the total flux compare to the pdf of the size-segregated fluxes? The results concerning the pdf of the wind friction velocity and of Q is very questionable. The "modelled" Q is computed after fitting a Weibull function on the experimentally determined U*.Why isn't it computed directly from the experimental wind friction velocity? The authors argued that the Weibull function fits "well" the U*pdf, but the quality of the fitting does not appear to be so good on figure 5: the number of wind speeds just above the threshold seems to be significantly underestimated while the highest winds seems to be overestimated by this function. Why not fitting only the values above the threshold or fitting U*3? This may improve the representation of the pdf and the quality of the modelled Q. The poor level of agreement between the computed and measured Qis also surprising since the

correlation between the modelled and measured Q was of 0.7 for the same experiment and the same model (Shao et al., 2011).

The pdf of the total flux is later shown in Fig. 5, but we now added this also to Fig. 4.

With Fig. 5, we try to understand the behavior of the pdfs of the saltation fluxes. Basically, qualitatively, the rapid drop of the probability of strong saltation is caused by that of u*. But, quantitatively, the model cannot reproduce the pdf. While this observation seems obvious, when we plotted the results, but still, the information is useful. We now followed the suggestions of the referee and have plotted additional fittings to the pdf of u*.

The poor level of agreement between the computed and measured Q is also surprising since the correlation between the modelled and measured Q was of 0.7 for the same experiment and the same model (Shao et al., 2011).

In Shao et al. (2011) only one event was studied, as by that time, the saltation fluxes was not completely computed for all events.

The discussion on the impact of the soil size distribution (page 8 lines 263-269) is not clear neither the conclusion that can be drawn. Could the impact of the soil size distribution on the modelled flux be estimated since it is an input data of the Shao's model?

These sentences are removed from the text to avoid confusion.

c) Intermittency: The "Intermittency section" should include a more precise description Interactive on the way it is computed. Indeed, the fact that it is as low as 0.1 when the threshold is comment 0.2m/s does not seem consistent with figure 1: for the well identified saltation events (days 56, 57, 60, 61, 62, 63, 69) the saltation flux Q1m looks positive when u* is higher than 0.2. A lower value suggest that the intermittency is computed over the whole time series, i.e. including periods of high winds with no saltation. Integrating periods of high winds with and without saltation does not corresponds to the initial concept on intermittency which correspond to the fact that during a given event, the wind velocity can be successively below or above the saltation threshold. From one event to the other many factors can act to prevent wind erosion on a given day compared to the others (precipitations, soil moisture). A table providing, event by event, the number of time steps with u*>u* cand the fraction of these time steps with Q>0 would make things more clear. The way the lower limit for Q is defined should also be described. Figure6 shows that the intermittency vary with the particle size and the authors conclude that the saltation of larger particle is more intermittent. An explanation could be the saltation threshold increases with the particle size (at least for particle diameter >80-100 m)

We understand the points the referee tried to make. We substantially reworked on this section, by introducing new definitions of intermittency. Our preference is to have some understanding of the statistic behavior of intermittency. We have therefore not focused on the intermittency of individual events, as we would end up with a lot of different values which would be difficult to interpret.

d) Power spectra: The power spectra of the saltation flux and of the wind friction velocity is one of the most interesting result of the manuscript. The way it is computed should be described and the results further discussed and analysed. It is quite common in the literature on turbulence to see normalized power spectrum of the wind velocity, including both the horizontal and the vertical components measured by nic anemometers. The frequency is also often normalized to the height of measurements and the mean wind speed, which allows to compare the results from different sites. Here the authors show the power spectrum of the wind friction velocity as a function of the frequency of measurements. They should explain why and how ACPD they produce the results from figure 7. How should the power spectrum of the wind friction velocity compare to the "classical" power spectrum of wind velocity?

The authors comment the behavior of the spectrum for different frequencies and relate this Interactive to the typical time scale of dynamical processes. References to similar results in terms comment of wind spectrum would make the results more convincing. The figure also raises the question of the data set of Q used to compute the power spectrum. The scale of the frequencies extend down to 10-6, i.e. more than 270 days while the whole sampling period is less than one month. From figure 1, it seems that the saltation episodes do not last longer than a day. Are the data set for Q1m and Q1s limited to periods for which the measured Q(z) are non-null (and once again the way the minimum Q is defined should be described) or do they include periods with no saltation recorded?

We have improve this section. As our sampling rate is relatively low, it is difficult to directly compute our u* spectrum with the Reynolds stress spectrum. We have nevertheless added references in which Reynolds shear stress spectra are shown. The frequency of 10^{-6} Hz corresponds to a period of 11.6 days. The time series of the data is about twice that length. The data points for which all sensors gave Q = 0 are included in the power spectra computation. The data points, for which no measurements were reported by the sensor were excluded in the computation. As the Q fluxes cover irregular time intervals, a non-uniform Discrete Fourier Transform (NDFT) is used. This is not a standard Matlab function, but we have tested that in the limit of regular time series our program delivers the some results. We are therefore confident that the power spectra analysis is correct.

The similarity of the spectrum of Q and U*is a strinking results that should be further highlighted. The power spectra of Q1m and Q1s both exhibit a peak at 2.10-3 Hz (less than 10 min). What does this mean? That a 1min acquisition time step is sufficient to properly describe the way saltation is impacted by turbulence? This is also an original results that should be further discussed.

The consistency between power spectra of Q_{1min} and Q_{1sec} at low frequency is expected, as Q_{1min} is derived from Q_{1sec}. We are not sure about the suggestion that "a 1min acquisition time step is sufficient to properly describe the way saltation is impacted by turbulence". What it shows is that one-minute sampling is sufficient to resolve the impact of very large eddies, but not turbulence.

Part 4.2 : The objective of this part is to test whether a probability distribution of u*t and c0 would improve the capability of the saltation model to reproduce the measured fluxes. This part also suffer for a lack of description on the method to estimate the pdf of ru*t and rc0 and on the way the modelled Q are finally computed for the final comparison with the measured Q. In this comparison, rather that the modelled and measured pdf of Q, one would expect a quantification of the benefit on the level of agreement between the measured and computed Q (correlation coefficients, RMSE, for example). It would be interesting also to test the change in the level of agreement with observations using the full distribution of the r parameters (figure 9) and the peak value only.

We have tried to clarify how rc0 and ru*t are computed. Yes. We have tried to use a full set of rc0 and rustar values to illustrate the improvement.

The author discuss the possible influence of the soil moisture, but the conclusion is not clear: the sentence "over the period .." does not seems to be correct (a verb missing ACPD ?) and cannot be understood. It is not clear from the following sentence ("in this study .;") whether the influence of the measured soil moisture is effectively accounted for in the modelled Q used to determine the distributions of r.

This is now clarified.

The discussion of the stochasticity of c0 in particular for weak saltation is not sufficiently linked to the discussion on the intermittency, which is mentioned only at the very end of the section.

We have tried to clarify

From figure 6, it is expected that u*t may vary with the particle size. But only rc0 is found dependent on particle size. The authors should comment on this possible contradiction. They state that the most frequent values of ru*t do not differ substantially, but what about the parameters of the distribution? And what range of variation is considered as substantial? When the author described thewayrc0is determined, it is not clear how they combine the determination of ru*t with the determination of rc0. Once again a more precise description should be given before the presentation and discussion the results.

We had some inaccurate descriptions re. ru*t close to the theoretic value. We have now modified the text. The dependency of rc0 on particle size is due to the different intermittency of different particle size groups. We have added some lines in the test about this,

In the last section, it should be clearly specified how the computation is made: are the measured u*t used? is the soil moisture effect included? are the "optimally estimated" u*t and c0 corrected with the p(u*t) and p(rc0)? If all these effects are included, what are the main sources of differences between the measured and modelled Q? Does the level of agreement between the modelled and measured pdfs of Q depend on the erosion events? What about the saltation flux cumulated for the different erosion events? Depending on the application, the error could be acceptable, but in any case, it should be quantified.

The effect of soil moisture has been considered. It is now clear that as the parameters u*t and c0 are distributed, a model using a fixed u*t and c0 cannot reproduce the measurements, but only "optimally" reproduce the measurements as defined by The absolute error, δQ_A, and Nash coefficient, I_{Nash}, which are used as measures for the goodness of the agreement between the model and the measurement. But major aspects of the measurements cannot be reproduced with deterministic u*t and c0, for example, the pdf of the Q fluxes.

Part5: Even if a few line of conclusion and perspective are given at the end of this section, I would suggest a to add more conclusive elements and some perspectives open by the presented work in terms of modelling but also in terms of improving the experimental setup for the coming field experiment.

Thanks for this comment. It makes good sense. We modified the conclusion section.

Minor comment:

Page1 line-38: Replace Staut by Stout.

We corrected the mistake.

Page2 line 68-69: It should be stated that, beside the establishment of the flux equations, the value of the coefficient is generally derived from measurements.

Accepted.

Page2 line 69-70: I would suggest to skip a line before the sentence “the total (all particle size) saltation flux :::”. Since the size dependence of the flux equation was not proposed by Kawamura (1964) nor White (1979) but was mainly added for modelling applications.

Page 2 line-75: I would suggest to skip a line before the sentence “Observations show, ..” and to add references from the literature to give a range of c0 derived from observations.

We did not do the separations, as we would otherwise ended up with several very short paragraphs. As to c0, we cannot give a range, as relatively few studies use the Kawamura scheme. We however added Gillette (1997) and Leys (1998) as references. Their data imply that c0 can vary over orders (may be two) in magnitude, as the data of Leys (1998) here show.

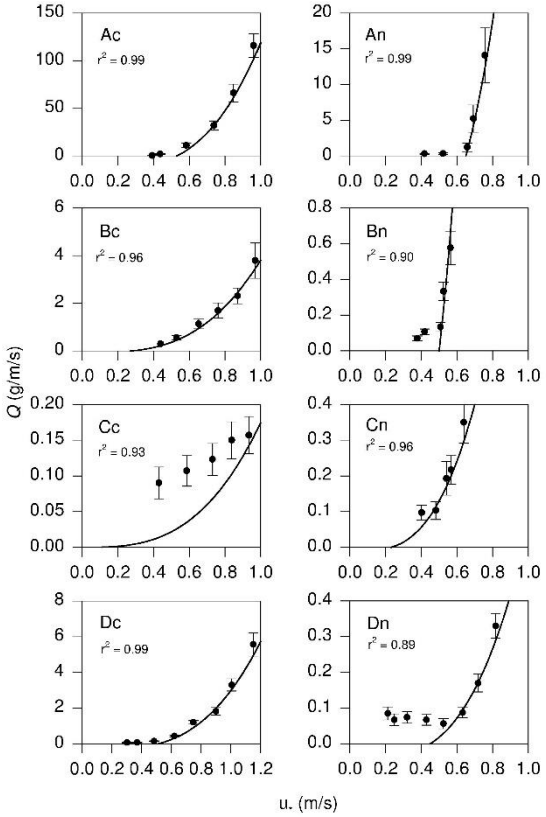

Figure R1: Fitting the Owen saltation model with observed data. The measurements were made on four soils with different textures denoted A, B, C and D, which corresponds to the U.S. taxonomy Aridosol (agrid), Aridosol (calic orthidf), Vertisol and Aridisol (haplargid). Two treatments were applied to each soil: bare uncultivated (denoted n) and bare cultivated (denoted c), giving a total of 8 soil-treatment combinations. The parameter r2 gives an indication for the goodness of the fitting with a perfect fit having a value of 1 (from Leys, 1998).

Page4 line 167-172. The temporal resolution of the atmospheric variable measurements should be given here.

Accepted

Page4 line 174-177: I am not sure it is the right place to present the wind erosion model.

This model has been discussed in detail in Shao (2011) and elsewhere. The relevant module consists basically Equations (1) – (3) already given I Section 1. We therefore think the information given is sufficient. In the revised draft, we say more explicitly that the

model used consists of Equations (1) – (3), and we added the sentences how particle size distribution is done.

Page7 figure 4, please specify Q1s and Q1m on the axes of the figure and use the scale for Q to make the two figures easily comparable.

Accepted.

Page 8, line 285-286. "This shows that saltation intermittency mainly occurs under weak wind conditions": since intermittency is defined as the fraction of time the wind friction velocity exceed the threshold, isn't it obvious that it occurs mainly when the wind friction velocity is close to the threshold?

We think it is nice that the data confirm what one would expect, but we are not sure without seeing the data that this is obvious, as intermittency must depends on the pdf of u_* near the surface. i.e., how turbulent flow is. We did not change anything in the text in this regard.

Page 10 line 318, part "4.2" should be part "3.2".

Thanks. Changed

Page 13, line 406-408: Figure 9 reports the distribution of r_{c0} and r_{u*t}, it does not show that "for a fixed choice of u_{*t} and co, even if they are optimally chose, a portion of the measurements cannot be represented by the model".

Thanks for this comment. A lot of changes have been made to this part of the text. We believe the concern of the referee is now adequately addressed.

Sincerely,

Yaping Shao
(on behalf of co-authors)

Turbulent Characteristics of Saltation and Uncertainty of Saltation Model Parameters

Dongwei Liu[1], Masahide Ishizuka[2], Masao Mikami[3], Yaping Shao[43]*

[1]School of Ecology and Environment, Inner Mongolia University, China
liudw@imu.edu.cn
[2]Faculty of Engineering, Kagawa University, Japan
ishizuka@eng.kagawa-u.ac.jp
[3]Office of Climate and Environmental Research Promotion, Japan Meteorological Business Support Center, Japan
mikami@jmbsc.or.jp
[43]Institute for Geophysics and Meteorology, University of Cologne, Germany
yshao@uni-koeln.de

Abstract: It is widely recognized that saltation is a turbulent process, similar to other transport processes in the atmospheric boundary layer. DBut due to the lack of high frequency observations, the statistic behavior of saltation is so far not well understood. In this study, we use the data from the Japan-Australian Dust Experiment (JADE) to investigate the turbulent characteristics of saltation by analyzing the probability density function, energy spectrum and intermittency of saltation fluxes. Threshold friction velocity, u_{*t}, and saltation coefficient, c_0, are two important parameters in saltation models, often assumed to be deterministic. ABut as saltation is turbulent in nature, we argue that it is more reasonable to consider them as parameters obeying certain probability distributions. The JADE saltation fluxes are used to estimate the u_{*t} and c_0 probability distributions. The stochasticity of these parameters is attributed to the randomness in friction velocity and threshold friction velocity as well as soil particle size.

Keywords: wind erosion; turbulent saltation; saltation intermittency; saltation model; threshold friction velocity; saltation coefficient; maximum likelihood

Highlight: We use the data from a field experiment to investigate saltation by analysing the probability density function, energy spectrum and intermittency of saltation fluxes. We also estimate two key wind-erosion model parameters and their probabilistic distributions. It continues the line of treating considering saltation as a turbulent process and represents a progress towards deriving more general wind erosion models.

1. Introduction

It is well-recognised known from the start of modern aeolian research [Bagnold, 1941] that saltation, the hoping motion of sand grains near the earth's surface, is a turbulent process [Bagnold, 1941]. However, early aeolian studies focused mainly on its "mean" behaviour. Most well-known is, for example, the Owen [Owen, 1964] saltation model which predicts that the vertically integrated saltation flux is proportional to u_* friction velocity cubed, where u_* is friction velocity, defined as $u_* = \sqrt{\tau / \rho}$ with τ being surface shear stress (N m^{-2}) and ρ air density (kg m^{-3}). A dedicated investigation on turbulent saltation was conducted by Butterfield [1991], which revealed the significant variability of saltation fluxes concealed in conventional time-averaged data. Stout and Zobeck [1997] introduced the idea of saltation intermittency and pointed out that even when the averaged u_* friction velocity, u_*, is below the threshold friction velocity, u_{*t}, saltation can still intermittently occur. The emphasis of the latter authors

Formatted: Superscript
Formatted: Superscript
Formatted: English (United States)
Formatted: para, Space Before: 12 pt, After: 14,4 pt, Pattern: Clear (Custom Color(RGB(252;252;252)))
Formatted: Font: Italic, English (United States)
Formatted: Font: Italic, English (United States), Subscript
Formatted: English (United States)
Formatted: Font: Italic, English (United States)
Formatted: Font: Italic, English (United States), Subscript
Formatted: English (United States)
Formatted: Font: (Default) Times New Roman, English (United States)
Formatted: Font: (Default) Times New Roman
Field Code Changed
Formatted: Font: (Default) Times New Roman
Formatted: Font: (Default) Times New Roman, Italic
Formatted: Font: (Default) Times New Roman
Formatted: Font: (Default) Times New Roman, English (United States)
Formatted: Font: (Default) Times New Roman, English (United States)
Formatted: Font: (Default) Times New Roman, English (United States), Superscript
Formatted: Font: (Default) Times New Roman, English (United States)
Formatted: Font: (Default) Times New Roman
Formatted: Font: (Default) Times New Roman, English (United States)
Formatted: Font: (Default) Times New Roman, English (United States)
Formatted: Font: (Default) Times New Roman, English (United States), Superscript
Formatted: Font: (Default) Times New Roman, English (United States)
Formatted: Font: (Default) Times New Roman
Formatted: English (United States)
Formatted: Font: Times New Roman, 12 pt, English (United States)
Formatted: Font: Times New Roman, 12 pt, English (United States)
Formatted: English (United States)
Formatted: English (United States)
Formatted: Font: Italic
Formatted: Font: Italic, Subscript
Formatted: English (United States)
Formatted: Font: Italic
Formatted: Font: Italic, Subscript
Formatted: English (United States)

emphasized ~~has been~~ on ~~the~~ saltation intermittency caused by ~~the~~ fluctuations of turbulent wind, but stochasticity of u_{*t} can also play a role. Turbulent saltation has attracted much attention in more recent years [e.g. McKenna Neuman et al. 2000; Davidson-Arnott and Bauer, 2009; Sherman et al. 2017] and large-eddy simulation ~~sophisticated~~ models have been under development ~~ed~~ to model the process [e.g. Dupond et al. 2013]. However, due to a ~~the~~ lack of high-frequency field observations of saltation fluxes, the statistical behaviour of turbulent saltation is, to date, not well understood.

A related problem is how saltation can be parameterized in wind erosion models. For example, for dust modelling, it is important to quantify saltation, as saltation bombardment is a main mechanism for dust emission. In wind erosion models, ~~threshold friction velocity, u_{*t},~~ is a key parameter which depends on many factors including soil texture, moisture, salt concentration, crust and surface roughness. In models, it is often expressed as

$$u_{*_t}(d;\lambda,\theta,s_l,c_r,\ldots) = u_{*_t}(d)\, f_\lambda(\lambda)\, f_\theta(\theta)\, f_{sl}(s_l)\, f_{cr}(c_r)\ldots \quad (1)$$

where $u_{*t}(d)$ is the minimal threshold friction velocity for grain size d [Shao and Lu, 2000]; λ is roughness frontal-area index; θ is soil moisture; s_l is soil salt content and c_r is a descriptor of surface crustiness; f_λ, $f_{\theta w}$, f_{sle} and f_{cr} are the corresponding correction functions. The corrections are determined semi-empirically, e.g., f_λ using the Raupach et al. [1993] scheme and $f_{\theta w}$ the Fécan et al. [1999] scheme. The corrections f_{sle} and f_{cr} are so far not well known.

For homogeneous saltation, the saltation flux can be computed using the Kawamura [1964] scheme, here multiplied by the fraction of erodible surface area σ_f,

$$Q(d) = \begin{cases} \sigma_f c_o \dfrac{\rho}{g} u_*^3 \left(1-\dfrac{u_{*t}}{u_*}\right)\left(1+\dfrac{u_{*t}}{u_*}\right)^2 & u_* > u_{*t} \\ 0 & u_* \le u_{*t} \end{cases} \quad (2)$$

where d is particle diameter in sand particle size range and ~~, ρ is air density,~~ g is acceleration due to gravity. ~~and u_* is friction velocity.~~ The saltation coefficient, c_0, is usually estimated empirically from field and/or wind-tunnel experiments. It falls between 1.8 and 3.1 a~~A~~ccording to Kawamura [1964], and is commonly set to 2.6 ~~the saltation coefficient, c_θ, falls between 1.8 and 3.1. In wind erosion models, c_θ is often set to 2.6~~ [White, 1979] in wind erosion models. The total (all particle sizes) saltation flux, Q, is a particle-size weighted average of $Q(d)$

$$Q = \int_{d_1}^{d_2} Q(d)\, p_s(d)\, \delta d \quad (3)$$

where d_1 and d_2 define the upper and lower limits of saltation particle size, respectively, and $p_s(d)$ is the soil particle size distribution. Observations show, however, $c_{0\theta}$ varies considerably from case to case (e.g. Gillette et al. 1997; Leys, 1998), and as the data presented later in this paper show, for a given location, it may vary from day to day and even during a wind erosion event.

While wind-erosion modules built in numerical weather and global climate models [e.g. Shao et al. 2011; Kok et al. 2014; Klose et al. 2014] are in general more sophisticated than what is described above and include a dust emission scheme, the estimate of Q is essentially done using

Formatted: English (United States)
Formatted: Font: Italic
Formatted: Font: Italic, Subscript
Formatted: English (United States)
Formatted: English (United States)
Formatted: English (United States)
Formatted: English (United States)
Formatted: English (United States)
Formatted: Font: Georgia, 13 pt, Font color: Gray-80%, English (United States), Expanded by 0,1 pt
Formatted: Subscript

Equations (1) to (3) or similar. Thus, the estimates of u_{*t} and specification of c_0 are ~~rather~~ critical to wind-erosion and dust modelling.

In most wind erosion models, both u_{*t} and $c_{0\phi}$ are treated as ~~considered to~~ being deterministic. ~~But a~~As saltation is turbulent, it is more rational to treat u_{*t} and c_o as parameters that ~~which~~ satisfy certain probability distributions. Saltation intermittency also implies that u_{*t} and c_0 ~~must~~ depend on the scale of averaging. Shao and Mikami [2005] noticed that u_{*t} for 10-minute averaged Q and 1-minute averaged Q are quite different. Namikas et al. [2003] and Ellis et al. [2012] have also noticed that averaging intervals of surface shear stress are important to quantifying sediment transport because both shear stress and saltation flux are turbulent.

Between 23 Feb and 14 Mar 2006, Ishizuka et al. (2008; 2014) carried out the Japan-Australian Dust Experiment (JADE) in Australia. In JADE, both u_* and Q, together with a range of atmospheric and soil surface quantities, were measured at relatively high sampling rates. The loamy sand soil surface at the JADE site was very mobile and thus the JADE data are representative to surfaces almost ideal for sand drifting. In this study, we analyse some aspects of the turbulent ~~statistic~~ behaviour of saltation using the JADE ~~field~~ measurements of saltation fluxes. In light of the analysis, we ask the question what the most likely values of u_{*t} and c_o are and how representative they are. We also estimate the probability distribution of the two parameters. ~~Between 23 Feb and 14 Mar 2006, Ishizuka et al. (2008; 2014) carried out the Japan-Australian Dust Experiment (JADE) on an Australian farm. In JADE, both u_* and Q, together with a range of atmospheric and soil surface quantities, were measured with high sampling rate. The loamy sand soil surface at the JADE site was very mobile and thus the JADE data are representative to surfaces almost ideal for sand drifting. The JADE data are used in this study.~~

2. Data and Method for Parameter Estimation ~~and Data~~

2.1 JADE Data

Ishizuka et al. carried out JADE between 23 Feb and 14 Mar 2006 on an Australian farm at (33°50'42.4"S, 142°44'9.0"E). The size of field is about 1 km in the E–W direction and about 4 km in the N–S direction. A range of atmospheric variables, land surface properties, soil particle-size distributions and size-resolved sand and dust fluxes were measured. During the study period, 12 wind-erosion episodes were recorded. The dataset is particularly valuable in that particle size resolved sand and dust fluxes [Shao et al. 2011] were measured. The details of the experiments and datasets can be found in Ishizuka et al. [2008, 2014] and hence only a brief summary is given here.

In JADE, three Sand Particle Counters (SPCs) [Yamada et al. 2002] were used to measure saltation at the 0.05, 0.1 and 0.3 m levels with a sampling rate of 1 Hz. A SLD (Super Luminescent Diode) light source is used to detect particles flying through the light beam. The frequency of the input signal is 1-30 kHz, implying that particles moving with speed less than 30 m s^{-1} can be detected. A SPC measures the saltation of particles in the range of 39 - 654 µm in 32 bins with mean diameters of 39, 54, 69 µm etc. with irregular increment ranging between 15 and 23 µm. At each measurement height, the saltation flux density (M L^{-2} T^{-1}), q, is obtained as the sum of q_j (saltation flux for size bin j) for the 32 size bins, i.e.

Formatted: Font: Bold

Formatted: Font: (Default) Times New Roman, 12 pt

Formatted: Font: (Default) Times New Roman, 12 pt

Formatted: Font: (Default) Times New Roman, 12 pt

Formatted: Font: (Default) Times New Roman, 12 pt

Formatted: Font: (Default) Times New Roman, 12 pt

Formatted: Font: (Default) Times New Roman, 12 pt

Formatted: Font: (Default) Times New Roman, 12 pt

Formatted: Font: (Default) Times New Roman, 12 pt

Formatted: Font: (Default) Times New Roman, 12 pt

Formatted: Font: (Default) Times New Roman, 12 pt, Superscript

Formatted: Font: (Default) Times New Roman, 12 pt

$$q = \sum_{j=1}^{32} q_j \quad (4)$$

The saltation flux, Q, is then estimated by integrating q over height, namely,

$$Q = \int q dz \quad (5)$$

In computing Q, we assume $q = q_0 \exp(-az)$ with q_0 and a being fitting parameters from the measurements. Prior to the field experiment, the SPCs were calibrated in laboratory and during JADE, they were checked in a mobile wind-tunnel at the site and compared with other saltation samplers. But as q was measured only at three heights, the vertical resolution of q is relatively poor and inaccuracies in the Q estimates are unavoidable, which we are unable to fully quantify. However, the profiles of q are well behaved and thus the inaccuracies in the absolute values of the Q estimates are not expected to be so large as to affect the conclusions of this study.

Q is computed using the SPC data at 1-second intervals. We denote its time series as Q_{1sec}. From Q_{1sec}, the one-minute averages, Q_{1min}, and 30-minute averages of saltation fluxes, Q_{30min}, are derived. All these quantities are also computed for individual particle size bins as

$$Q_j = \int q_j dz \quad (5a)$$

Atmospheric variables, including wind speed, air temperature and humidity at various levels, as well as radiation, precipitation, soil temperature and soil moisture were measured using an automatic weather station (AWS). These quantities were sampled at 5-second intervals and their averages over 1-minute intervals were recorded. Two anemometers were mounted at heights 0.53 m and 2.16 m on a mast for measuring wind speed. Also available are the Monin-Obukhov length and sensible heat fluxes. From the wind measurements, surface roughness length z_0 and friction velocity u_* are derived, assuming a logarithmic profile (with stability correction) of the mean wind. The roughness length for the experiment site is estimated to be 0.48 mm.

Friction velocity is computed with 1-minute averaged wind data, denoted as u_{*1min}, and 30-minute averaged wind data, denoted as u_{*30min}. In atmospheric boundary-layer studies, there is no standard for how long one should average wind to "correctly" estimate u_*, but it is common to average over 10 to 30 minutes. But how long one averages depends on the purpose of the averaging. If u_* is used as a scaling velocity for the atmospheric boundary layer, e.g., as measure of turbulence intensity, it is necessary to average over a sufficiently large time interval to obtain a "constant" u_*. In this paper, u_* is a surrogate of shear stress, the variation of which drives that of saltation. Therefore, short averaging times are preferred, subject to that they are larger than the response time of aeolian flux to shear stress. Anderson and Haff (1988) and Butterfield (1991) suggested that this response time is of order of one second.

Observations of surface soil properties, including soil temperature and soil moisture, were made at 1-minute intervals. The surface at the JADE site was relatively uniform. A survey of ground cover over an area of 900 x 900 m^2 at the site was made on 11 March 2006. The area was divided into 9 tiles and surveyed along one transect of 300 m long in each tile. Photographs were taken every 5 m by looking down vertically to a point on the ground. Surface cover was estimated to be ~ 0.02 (see Appendix of Shao et al. 2011).

Field Code Changed
Field Code Changed
Formatted: Font: Italic
Field Code Changed
Formatted: Font: (Default) Times New Roman
Formatted: Font: (Default) Times New Roman
Formatted: Font: (Default) Times New Roman, Italic
Formatted: Font: (Default) Times New Roman, Italic, Subscript
Formatted: Font: (Default) Times New Roman
Formatted: Font: Italic
Formatted: Font: Italic, Subscript
Formatted: Font: (Default) Times New Roman
Formatted: Font: (Default) Times New Roman
Formatted: Font: (Default) Times New Roman
Formatted: Font: (Default) Times New Roman
Formatted: Font: (Default) Times New Roman
Formatted: Font: (Default) Times New Roman
Formatted: Font: (Default) Times New Roman
Formatted: Font: (Default) Times New Roman, Italic
Formatted: Font: (Default) Times New Roman, Italic, Subscript
Formatted: Font: (Default) Times New Roman
Formatted: Font: (Default) Times New Roman, Italic
Formatted: Font: (Default) Times New Roman, Italic, Subscript
Formatted: Font: (Default) Times New Roman
Formatted: Font: (Default) Times New Roman
Formatted: Font: (Default) Times New Roman
Formatted: Font: (Default) Times New Roman
Formatted: Font: (Default) Times New Roman
Formatted: Font: (Default) Times New Roman
Formatted: Font: (Default) Times New Roman
Formatted: Font: (Default) Times New Roman
Formatted: Automatically adjust right indent when grid is defined, Line spacing: At least 10,5 pt, Adjust space between Latin and Asian text, Adjust space between Asian text and numbers
Formatted: Superscript

The wind erosion model, as detailed in Shao et al. (2011), is used for computing the saltation fluxes using the JADE atmospheric and surface soil measurements as input. The saltation model component is as described in Section 1, consisting of Equations (1) – (3). The fraction of erodible surface area, σ_f, used in Equation (1), is one minus the fraction of surface cover. The soil particle size distribution (psd), $p_s(d)$, required for Equation (3), is based on soil samples collected at the JADE site and analyzed in laboratory. The analysis was done using a Microtrac (Microtrac MT3300EX, Nikkiso Co. Ltd.), a particle size analyzer based on laser diffraction light scattering technology. Water was used for sample dispersion. Depending on the methods (pretreatment and ultrasonic vibration) used, the soil texture can be classified as sandy loam (clay 0.3%, silt 25% and sand 74.7%) or loamy sand (clay 11%, silt 35% and sand 54%). The sandy loam psd is used in this study, which has a mode at ~180 μm (see Shao et al. 2011, Fig. 5, Method A).

The default value of c_0 is set to 2.6, as widely cited in the literature [e.g. White, 1979] and the default value of u_{*t} is computed using Equation (1) with $u_{*t}(d)$ computed using the Shao and Lu [2000] scheme, f_λ using the Raupach et al. [1993] scheme, f_θ the Fécan et al. [1999] scheme, and f_{sl} and f_{cr} set to one. The frontal area index λ and soil moisture θ are both observed data from JADE.

2.2 Method for Parameter Estimation

Different choices of c_0 and u_{*t} would lead to different model-simulated saltation fluxes which may or may not agree well with the measurements. By fitting the simulated saltation fluxes to the measurements, we determine the optimal estimates of c_0 and u_{*t} and the probability density function (pdf) of these parameters. The method based on the Bayesian theory is used for the purpose.

Suppose $\tilde{X} = (\tilde{x}_1, \tilde{x}_2, ..., \tilde{x}_n)$ is a measurement vector, with $\tilde{x}_i$ being the measured value at time t_i, and A is a model with a forcing vector F and model parameter vectors ~~β~~ β. Let the initial state of the system be i_0, then the modelled value of the system, $X = (x_1, x_2, \ldots, x_n)$, can be expressed as

$$X(\beta) = A(i_0, F; \beta) \qquad (64)$$

The error vector is given by $E(\beta) = \tilde{X} - X$, here, fully attributed to β. Given $\tilde{x}$, the posterior parameter pdf ~~probability density function (pdf)~~, $p(\beta|\tilde{X})$, can be estimated from the Bayes theorem:

$$p(\beta|\tilde{X}) \propto p(\beta)\, p(\tilde{X}|\beta) \qquad (75)$$

where $p(\beta)$ is the prior parameter pdf and~~,~~ $p(\tilde{X}|\beta)$ the likelihood. If $p(\beta)$ is given, then the problem of finding $p(\beta|\tilde{X})$ reduces to finding the maximum likelihood. Assuminge the error residuals are independent and Gaussian distributed with constant variance, σ^2, the likelihood can be written as

$$p(\tilde{X}|\beta) = \prod_{i=1}^{n} \frac{1}{\sqrt{2\pi}\sigma} \exp\left(-\frac{(x_i - \tilde{x}_i)^2}{2\sigma^2} \right) \qquad (86)$$

Formatted: Automatically adjust right indent when grid is defined, Adjust space between Latin and Asian text, Adjust space between Asian text and numbers

Formatted: Font: Italic

Formatted: Font: Italic, Subscript

Formatted: Font: Italic

Formatted: Not Highlight

Formatted: Font color: Auto

Formatted: Not Highlight

Formatted: Not Highlight

Formatted: Not Highlight

Formatted: Not Highlight

Formatted: Justified

Formatted: Font: Italic

Formatted: Font: Italic

Formatted: Font: Italic, Subscript

Formatted: Font: 12 pt

In this case, maximizing the likelihood is equivalent to minimizing the error, i.e.,

$$R^2(\beta) = \min \sum_i (x_i - \tilde{x}_i)^2 \qquad (9)$$

The solution of Equation (9) gives an optimal (i.e. with maximum likelihood) estimate of mean ~~This is the least-squares method for estimating β, $\tilde{x}$.~~ This is the popular least-squares method. A disadvantage of the method is that it assumes a Gaussian posterior parameter pdf and the computing the β variance requires the pre-knowledge of the accuracy of the data.

As an alternative, the approximate Bayesian computation (ABC) method has been proposed [e.g. Vrugt and Sadegh, 2013]. It is argued that a parameter value β^* should be a sample from $p(\beta|\tilde{X})$ as long as the distance between the observed and simulated data is less than a small positive value

$$\rho(\beta^*) = \left| X(\beta^*) - \tilde{X} \right| \le \varepsilon \qquad (10)$$

This procedure provides explicitly an estimate of parameter pdf ~~the probability distribution function~~ for given dataset. The ABC method is numerically simple: from a prior pdf (e.g. uniform) of β a β^* is stochastically generated and the model is run. If Equation (10) is satisfied, then β^* is accepted or otherwise rejected. This procedure is repeated and the a-priori pdf of β is mapped to a posterior pdf of β. The ABC method has the disadvantage though that it is numerically inefficient. More efficient techniques based on the same principle exist, e.g., Markov Chain Monte Carlo Simulation [Sadegh and Vrugt, 2014]. In this study, we apply the Differential Evolution Adaptive Metropolis (DREAM) algorithm proposed by Vrugt et al. (2011) for estimation of hydrologic model parameters. The algorithm integrates Differential Evolution [Storn and Price, 1997] and self-adaptive randomized subspace sampling to accelerate a Markov Chain Monte Carlo simulation. A full description of the DREAM algorithm is beyond the scope of our study. Interested readers should refer to the above cited references for details.

~~Ishizuka et al. carried out JADE between 23 Feb and 14 Mar 2006 on an Australian farm at (33°50'42.4"S, 142°44'9.0"E). A range of atmospheric variables, land surface properties, soil particle size distributions and size resolved sand and dust fluxes are measured. During the study period, 12 wind erosion episodes occurred. The dataset is particular valuable in that particle size resolved sand and dust fluxes [Shao et al. 2011] were measured. The details of the experiments and datasets can be found in Ishizuka et al. [2014] and hence only a brief summary is given here.~~

~~In JADE, three Sand Particle Counters (SPCs) [Yamada et al. 2002] were used to measure saltation at the 0.05, 0.1 and 0.3 m levels with a sampling rate of 1 Hz. A SPC measures the saltation of particles in the range of 38.9 - 654.3 μm in 32 bins with mean diameters of 38.9, 54.1, 69.2 μm etc. At each measurement height, the saltation flux density ($ML^{-2}T^{-1}$), q, is obtained as the sum of q_i (saltation flux for size bin i) for the 32 size bins, i.e.~~

~~$$q = \sum_{j=1}^{32} q_j \qquad (11)$$~~

~~The saltation flux, Q, is then estimated by integrating q over height, namely,~~

Formatted: Justified
Formatted: Font: Not Italic
Formatted: Font: Not Italic
Formatted: Font: Italic
Formatted: Superscript

~~$Q = \int q dz$ (12)~~

~~In computing Q, we assume $q = q_0 \exp(-\alpha z)$ with q_0 and α being fitted from the measurements. As q was measured only at three heights, the vertical resolution of q is relatively poor and inaccuracies in the Q estimates are unavoidable. However, the profiles of q are well behaved and thus the inaccuracies in the Q estimates are not expected to be so large to affect the conclusions of this study.~~

~~Atmospheric variables, including wind speed, air temperature and humidity at various levels, as well as radiation and precipitation, were measured using an automatic weather station (AWS). Two anemometers were mounted at heights 0.53m and 2.16m on a mast for measuring wind speed. Also available are the Monin-Obukhov length and sensible heat fluxes. From the wind measurements, surface roughness length z_0 and friction velocity u_* are derived, assuming a logarithmic profile (with stability correction) of the mean wind. The roughness length for the experiment site is estimated to be 0.48 mm. Observations of surface soil properties, including soil temperature, soil moisture and surface cover were also made. The wind erosion model, as detailed in Shao et al. (2011), is used for computing the saltation fluxes using the JADE atmospheric and surface soil measurements as input. The essence of the saltation model component is as described in Section 1. The fraction of erodible surface area, σ_f, used in Equation (1), is estimated from photos using the technique as detailed Shao et al. (2011). For the site, the fraction of surface cover is about 0.02, almost negligible.~~

~~The resolution of Q is one second. We denote its time series as Q_{1s}. From Q_{1s}, the one-minute averages, Q_{1m}, and 30-minute averages of saltation fluxes, Q_{30m}, are derived. The resolution of friction velocity is one minute. We denote the one-minute averages of friction velocity as u_{*1m} and the 30-minute averages u_{*30m}.~~

3. Statistical Features of Saltation ~~Results~~

3.1 Time Series~~Statistical Features of Saltation~~

To provide an overview of the dataset used in this study. Fig. 1a shows the time series of Q_{1min} and u_{*1min}, and Fig. 2 Q_{30min} and u_{*30min}. During the 20-day period, aeolian sand drift occurred almost every day at the site according to the field logging book, but only 12 events were recorded using the SPCs. Saltation fluxes were not measured on Day 55, 58, 59, 64 and then Day 66 to 70, due to either instrument maintenance or use of the SPCs for other purposes (e.g. wind-tunnel experiments). The figures show that both Q and u_* fluctuate significantly –and saltation is turbulent. Fig. 1b shows an enlarged plot of the Q_{1min} and u_{*1min} time series for Day 61 and 62. At the JADE site, u_{*t} was about 0.2 m s^{-1}. On Day 61, u_* was mostly larger than this value and saltation was almost continuous, while on Day 62, u_* was close to this value and weak saltation occurred frequently also when u_* was below 0.2 m s^{-1}~~fluctuate~~. , –Fig. 2b is as Fig.1b, but for Q_{30min} and u_{*30min}. A comparison of Fig. 1b and Fig. 2b reveals that ~~but~~ the amplitude of the Q_{1min} fluctuations is several times of that of the Q_{30min} fluctuations. A strong correlation between the time series of Q_{30min} and u_{*30min} can be directly seen in Fig. 2b.

Formatted: Normal, Don't adjust right indent when grid is defined, Don't adjust space between Latin and Asian text, Don't adjust space between Asian text and numbers

Formatted: Font: Italic
Formatted: Font: Italic, Subscript
Formatted: Superscript
Formatted: Font: Italic
Formatted: Font: Italic, Subscript
Formatted: Font: Italic
Formatted: Font: Italic, Subscript
Formatted: Font: Italic
Formatted: Font: Italic, Subscript
Formatted: Superscript
Formatted: Font: Italic
Formatted: Font: Italic, Subscript
Formatted: Font: Italic
Formatted: Font: Italic, Subscript

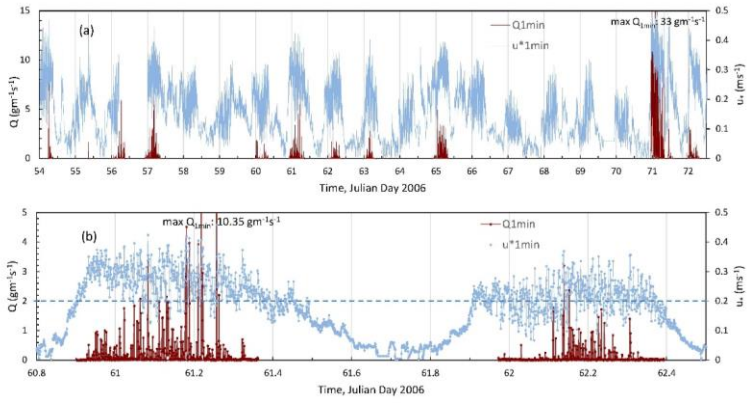

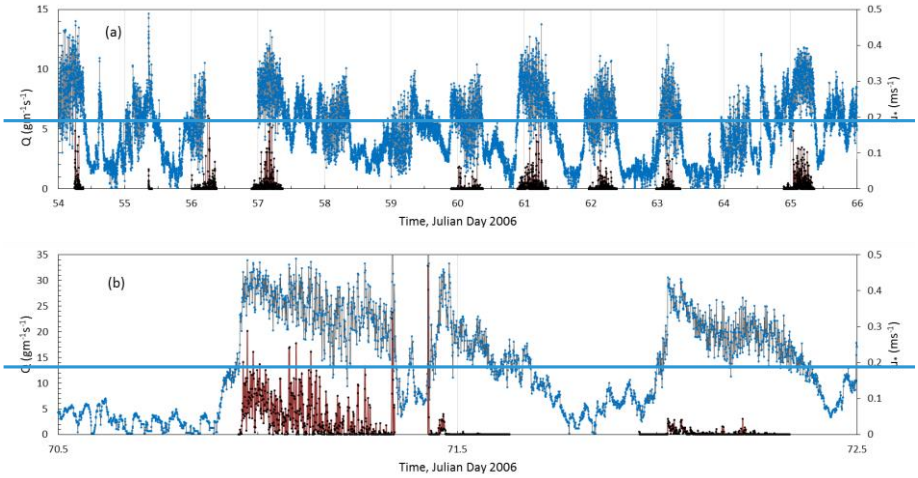

Figure 1: (a) Observed time series of 1-min averaged saltation flux, Q_{1min} (g m^{-1}s^{-1}), and friction velocity, $u*_{1min}$ (m s^{-1}), for the JADE study period; (b) an enlarged plot of (a) for the erosion events on Day 61 and 62. Note that the axes in (b) have different scales than as in (a).

Formatted: Justified

Formatted: Subscript

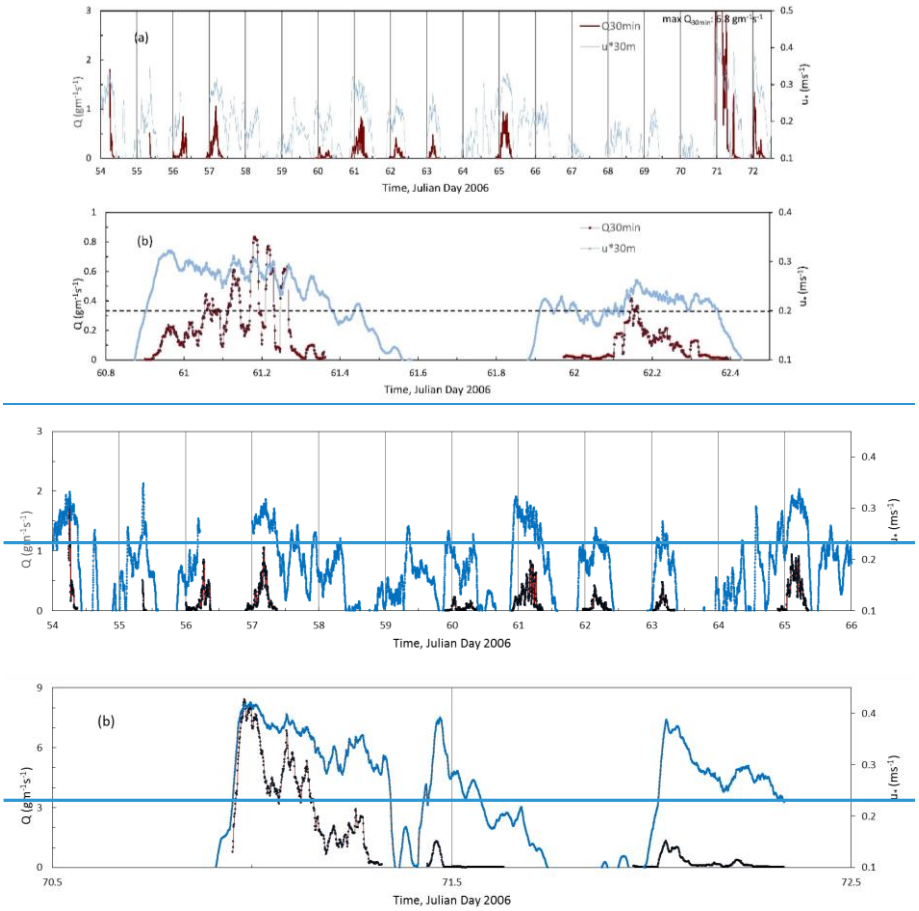

Figure 2: As Fig. 1, but for running means over 30-min intervals.

In Fig. 3a, b and c, Q is plotted against u_*^3. Several interesting features can be identified. For the majority of the points, the $Q \sim u_*^3$ relationship appears to hold, but this relationship can vary significantly even for the same data set from event to event. For example, large differences exist between days 70 and 71 ~~62~~ (denoted D70-71, an event ~~day~~ of intensive wind erosion) and Day ~~day~~ 72 (a day of weak wind erosion), as seen in both Fig. 3a and Fig. 3b. ~~Also hysteresis can be observed in the saltation flux and friction velocity relationship (Fig. 3c): during an erosion event, for the same friction velocity, saltation is much stronger in the strengthening than in the weakening phase.~~ There may be many likely reasons for the differences ~~hysteresis in~~ the $Q \sim u_*$ relationship ~~between sediment flux and friction velocity~~ but the most conspicuous ~~likely~~ are ~~the~~ differences in atmospheric turbulence (e.g., ~~more~~ gustiness ~~in the strengthening than in the weakening phase~~) and time-varying surface conditions (e.g. particle sorting and aerodynamic roughness). Fig. 3d shows the time series of (u_{*1min}–u_{*30min}), a measure of turbulent fluctuations. It is seen that saltation is associated with not only high surface shear stress but also high shear stress fluctuations. The large difference in the $Q \sim u_*$ relationship between D70-71 and D72

Formatted: Normal
Formatted: Font: Italic
Formatted: Font: Italic
Formatted: Font: Italic, Subscript
Formatted: Font: Italic
Formatted: Font: Italic, Subscript
Formatted: Font: Italic
Formatted: Font: Italic, Subscript
Formatted: Font: Italic
Formatted: Font: Italic
Formatted: Font: Italic, Subscript

(Fig. 3b) is probably attributed to the strong differences in turbulent fluctuations (Fig. 3d): D70-71 was a hot gusty day with top (2 cm) soil temperature reaching 53ºC, while D72 was cooler and less gusty with soil temperature 5ºC lower. Also hysteresis is observed in the Q~u_* relationship, as shown in Fig. 3c, using D71 and D72 as example. Fig. 3d shows that for all three events selected (D70-71, D71 and D72), saltation has a relatively short (0.5 to 2 hours) strengthening phase, followed by a longer weakening phase. During an erosion event, for the same u_*, saltation is stronger in the strengthening than in the weakening phase. An examination of Fig. 3d suggests that the hysteresis cannot be simply attributed to the intensity of turbulence. We speculate that it is probably more related to flow-saltation feedbacks (e.g. stronger splash entrainment in the strengthening phase) and the modification of surface aerodynamic conditions (e.g. particle sorting and reduced surface roughness Reynolds number).

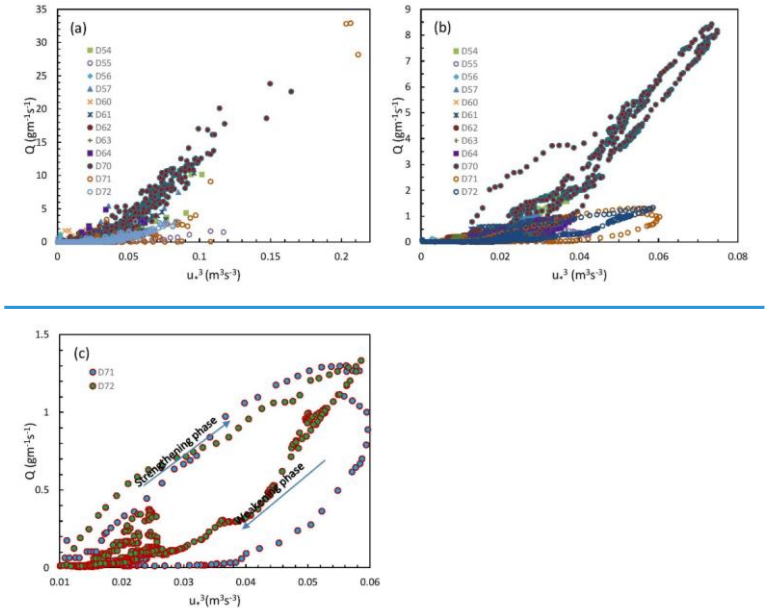

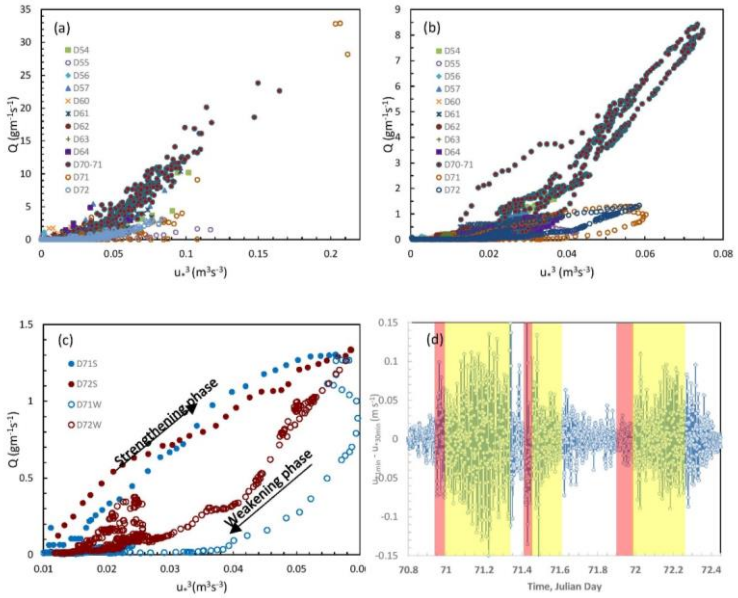

Figure 3: (a) Saltation flux, Q (g m^{-1} s^{-1}), plotted against friction velocity, u_*^3 (m^3 s^{-3}), for 1-minute averages; (b) As (a), but for 30-minute averages; (c) As (b), but enlarged to illustrated saltation hysteresis on D71 and 72; D71S/72S denote the strengthening and D71W/72W the weakening phase of the D71/72 event; (d) Time series of μ_* derivations, given by ($\mu_{*1min} - \mu_{*30min}$), for D70-71, D71 and D72. The strengthening phase is marked red and the weakening phase yellow. ~~.~~

3.2 Probability Density Function of Saltation Fluxes

How well the saltation model performs, whether u_{*t} and c_o are universal and how they are probabilistically distributed must depend on the turbulent properties of saltation. As the JADE saltation fluxes are sampled at 1 Hz, we can use these data to examine ~~reveal~~ (to some degree) the statistical behavior of saltation. In Fig. 4, the pdfs of the saltation fluxes for different particle size groups are plotted, computed using Q_{1sec} and Q_{1min}. It is seen that the pdfs generally behaves as~~like~~

$$p(Q) \propto Q^{-\alpha} \qquad (11\text{~~3~~})$$

In case of Q_{1sec}, there seems to be a distinct change in α at a critical value of $Q_c \sim 3$ g m^{-1} s^{-1}, with α ~ 1 ~~= 0.8 ~ 0.9~~ for $Q < Q_c$ and α ~ ~~=~~ 4~~.0~~ for $Q > Q_c$. The pdfs derived from Q_{1min} appear to follow ~~be somewhat different, although~~ the basic functional form of ~~is as given by~~ Equation (11~~3~~). Again, ~~In this case,~~ α is about 1 and tends to be larger ~~drops off to about 2~~ for large Q values. Fig. 4 shows that the pdfs of Q depend~~s~~ ~~quite~~ significantly on the interval of time averaging, i.e., ~~. Fig. 4 also shows that~~ after averaging, smaller saltation fluxes become more frequent~~likely~~. This is because the time series of Q_{1sec} is more intermittent (see also Fig. 6).

Formatted: Font: Italic
Formatted: Font: Italic, Subscript
Formatted: Font: Italic
Formatted: Font: Italic, Subscript
Formatted: Font: Italic
Formatted: Font: Italic, Subscript
Formatted: Font: Italic

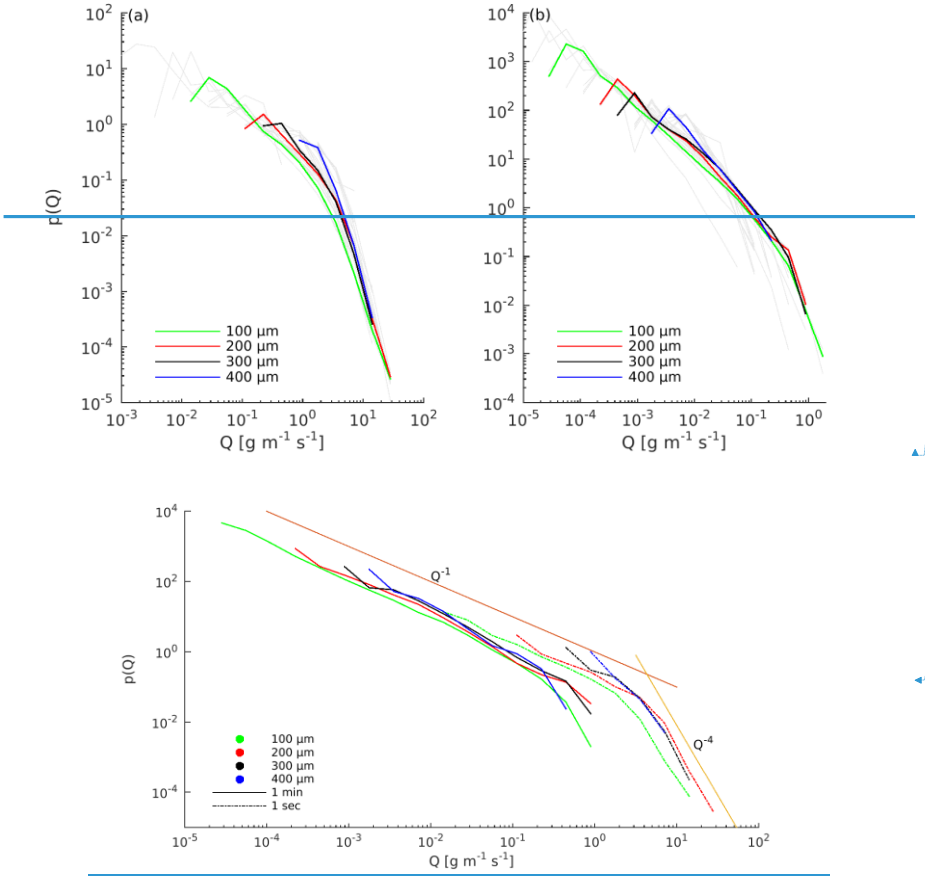

Figure 4: ~~(a)~~ Probability density functions of Q_{1sec} (solid lines) and of Q_{1min} (dashed lines) for four different particle sizes. Two additional lines $p(Q) \sim Q^{-1}$ and Q^{-4} are drawn as reference. ~~saltation flux averaged over 1 second; (b) as (a), but for saltation fluxes averaged over 1 minute.~~

The pdfs of Q_{1sec} and Q_{1min} integrated over all particles are shown in Figure 5b. Again, the pdfs show the general behavior of $p(Q) \sim Q^{-1}$. In theory, $p(Q)$ can be derived from the pdf of u_*, $p(u_*)$. From Equation (2), we have

$$\frac{dQ}{du_*} = c_0 \frac{\rho}{g}\left(3u_*^2 + 2u_* u_{*_t} - u_{*_t}^2\right) \quad \text{for} \quad u_* > u_{*_t} \qquad (124)$$

This can be used to obtain ~~It follows that~~

Formatted: English (United States)

Formatted: Centered

Formatted: Font: Italic

Formatted: Font: Italic, Subscript

Formatted: Font: Italic

Formatted: Font: Italic, Subscript

Formatted: Font: Italic

Formatted: Font: Italic

Formatted: Font: Italic

Formatted: Superscript

Formatted: Font: Italic

Formatted: Superscript

$$p(Q) = \begin{cases} p(u_*)\dfrac{du_*}{dQ} & \text{for} \quad u_* > u_{*_t} \\ 0 & \text{for} \quad u_* \le u_{*_t} \end{cases} \qquad (135)$$

Fig. 5a shows the $p(u_*)$ estimated from u_{*1min} together with the fitted Weibull distribution. For the fitting, emphasis is made to ensure that $p(u_*)$ for $u_* > 0.2$ ms^{-1} is best approximated. ~~and~~ Fig. 5b shows the $p(Q)$ estimated from Q_{1min}. ~~It is seen that $p(u_*)$ can be well fitted with a Weibull distribution.~~ We computed $p(Q)$ using Equation (135) with the fitted $p(u_*)$, assuming $u_{*t} = 0.2$ ms^{-1} and $c_0 = 2.6$. It is seen that ~~while~~ the observed and modelled $p(Q)$ ~~only~~ have qualitative similarities (namely $p(Q)$ decreases with increasing Q) but using Equations (12) and (13) we ~~are profoundly different. Fig. 5 shows that even if the saltation model~~ cannot well reproduce the observed $p(Q)$ ~~if u_{*t}.~~ For example, the model fails to predict the lowly frequent strong saltation fluxes and fails to predict the highly frequent ~~-~~weak saltation occurring when u_* is below the specified threshold. Tests using several smaller u_{*t} values (0, 0.05 and 0.1). With smaller u_{*t} values, the highly frequent weak saltation fluxes are better reproduced, but fra from satisfactory.

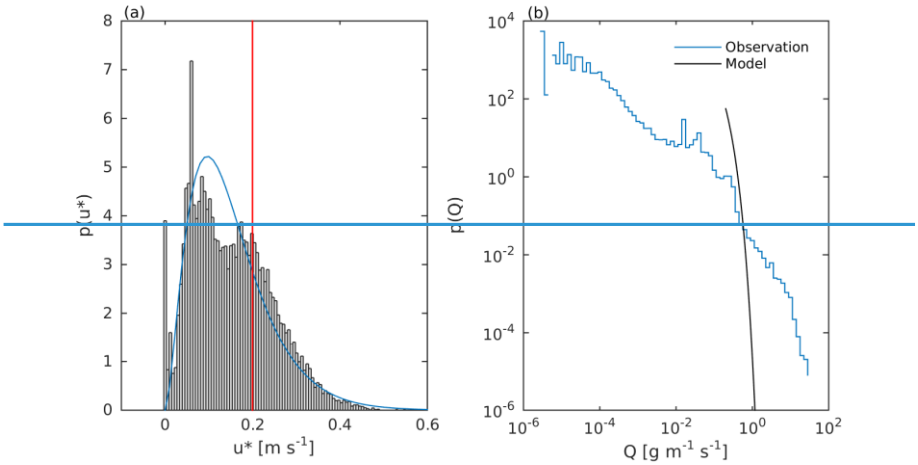

Formatted: Font: Italic
Formatted: Font: Italic
Formatted: Font: Italic, Subscript
Formatted: Font: Italic
Formatted: Font: Italic, Subscript
Formatted: Superscript
Formatted: Font: Italic
Formatted: Font: Italic
Formatted: Font: Italic
Formatted: Font: Italic
Formatted: Font: Italic, Subscript
Formatted: Font: Italic
Formatted: Font: Italic, Subscript
Formatted: English (United States)

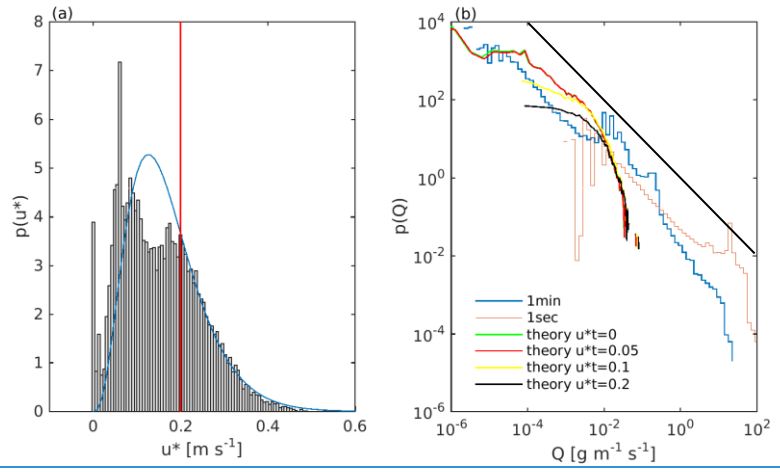

Figure 5: (a) Probability density functions of friction velocity, $p(u_*)$, plotted against u_* (bars). To compute $p(u_*)$, u_{*1min} is used; a Weibull distribution (blue line) is fitted to $p(u_*)$; the red line marks the assumed threshold friction velocity. (b) Probability density function of Q, $p(Q)$, estimated using Q_{1min} (blue) and Q_{1sec} (dark red) and using Equation (135) assuming several u*t values (u_{*t} = 0.0 m s^{-1}, green; 0.05 m s^{-1}, red; 0.1 m s^{-1}, yellow; 0.2 m s^{-1}, black). The $p(Q) \sim Q^{-1}$ line is also drawn for comparison.

Also, the soil particle size distribution can influence $p(Q)$. In JADE, soil samples from the experiment site were collected and the psds were analyzed in laboratory. Depending on the methods used, the soil texture can be classified as sandy loam (clay 0.33%, silt 25% and sand 74.67%) or loamy sand (clay 11%, silt 35% and sand 54%). The soil at the observation site is bimodal with one psd maximum at about 180 μm and another at about 500 μm (not shown). The relatively large $p(Q)$ at about $Q_{1m} = 10^{-1}$ gm^{-1}s^{-1} is related to the psd maximum at d = 180 μm.

3.3 Saltation Intermittency

Following Stout and Zobeck [1997], the intermittency of saltation, γ_{int}, is defined as the fraction of time during which saltation occurs at a given point in a given time period. It should be pointed out that as saltation is a turbulent process, saltation intermittency describes only the behaviour of the process at $u_* \sim u_{*t}$, i.e., saltation intermittency is merely a special, although important, case of turbulent saltation. Several formulations of γ are possible. Stout and Zobeck [1997] The latter authors assumed that saltation is expected to occurs only in the time windows when u_*friction velocity exceeds the u_{*t}threshold friction velocity. Therefore, if suppose $p(u_*)$ is known, then γ_{int} for a given u_{*t} can be estimated as is

$$\gamma_a(u_{*t}) = 1 - \int_0^{u_{*t}} p(u_*)du_* \quad \gamma_a = 1 - \int_0^{u_{*tc}} p(u_*)du_* \qquad (14a)$$

This definition of γ_{int} is problematic, because u_{*t} here is fixed. Stout and Zobeck [1997] used the counts per second of sand impacts on a piezoelectric crystal saltation sensor as a measure of saltation activity and found that $\gamma_{a\,int}$ rarely exceeded 0.5.

Formatted: Font: Italic
Formatted: Font: Italic, Subscript
Formatted: Font: Italic
Formatted: Font: Italic, Subscript
Formatted: Superscript
Formatted: Superscript
Formatted: Superscript
Formatted: Superscript
Formatted: Font: Italic
Formatted: Font: Italic
Formatted: Superscript
Formatted: Highlight
Formatted: English (United States)
Formatted: Font: Italic
Formatted: Font: Italic
Formatted: Font: Italic, Subscript
Formatted: Font: Italic
Formatted: Font: Italic, Subscript
Formatted: Font: Italic
Formatted: Font: Italic
Formatted: Font: Italic, Subscript

~~This definition of γ_{int}~~ In Equation (14a) ~~is problematic, because u_{*t} here~~ is fixed and thus saltation intermittency is attributed entirely to the fluctuations of u_*. In reality, u_{*t} also fluctuates and satisfies certain pdfs (Raffaele et al., 2016). In analogy to Equation (14a), γ for a given u_* can be estimated as~~:~~

$$\gamma_b(u_*) = 1 - \int_{u_*}^{\infty} p(u_{*t})du_{*t} \qquad (14b)$$

More generally, we can define saltation intermittency as

$$\gamma_c = \int_0^{\infty}\left[1 - \int_0^{u_{*t}} p(u_*)du_*\right]p(u_{*t})du_{*t} = \int_0^{\infty} \gamma_a(u_{*t})p(u_{*t})du_{*t} \qquad (14c)$$

or

$$\gamma_c = \int_0^{\infty}\left[1 - \int_{u_*}^{\infty} p(u_{*t})du_{*t}\right]p(u_*)du_* = \int_0^{\infty} \gamma_b(u_*)p(u_*)du_* \qquad (14d)$$

Equations (14c) and (14d) reduce to Equation (14a) in case of $p(u_{*t}) = \delta(u_{*t})$ and to Equation (14b) in case of $p(u_*) = \delta(u_*)$, respectively.

The computation of saltation intermittency function $\gamma_a(u_{*t})$ is done by integrating $p(u_{*t})$ (Fig. 5a) to fixed value of u_{*t}. In Fig. 6a, γ_a as function of u_{*t} is plotted. The behaviour of $\gamma_a(u_{*t})$ is as expected: it is one at $u_{*t} = 0$ and decreases to zero at about $u_{*t} = 0.5$ ms^{-1} as in the case of JADE, u_* rarely exceeded this value. For $u_{*t} = 0.2$ ms^{-1}, γ_a is 0.35, comparable with the result of Stout and Zobeck (1997) who reported an intermittency of 0.4. As $p(u_{*t})$ is not known, Equation (14b) cannot be used directly, but we can ~~We~~ compute ~~examined~~ $\gamma_{b}(u_*)$ ~~$_{int}$~~ using the JADE data. First, it γ_{int} is computed using Q_{1min} ~~c~~, ~~onditionally sampled~~ This is done ~~for $u_* > u_{*c}$ with u_{*c} successively varied from small to large,~~ by selecting a fixed u_* say u_{*c}, and counting the time fraction, T_{u*}, which satisfies $|u_* - u_{*c}| < \delta$, (used is $\delta = 0.05$ ms^{-1}) and the time fraction, T_{Q1min}, which satisfies $|u_* - u_{*c}| < \delta$ and $Q_{1min} > 0$. By definition, saltation intermittency is T_{Q1min}/T_{u*}. ~~with~~ The value u_{*c} is successively increased to obtain saltation intermittency function $\gamma_b(u_*)$, ~~u_{*c} successively varied from small to large.~~ as plotted in ~~In~~ Fig. 6a. ~~, γ_{int} is plotted as a function of u_{*c}.~~ It is seen that for Q_{1min}, ~~on one-minute intervals,~~ $\gamma_{bint}(u_*)$, increases from about 0.6 at u_* ~ 0.1 ms^{-1} to about one at u_* = 0.3 ms^{-1}, ~~has a maximum of about 0.25 for small u_{*c} and decreases to zero at about u_{*c} = 0.3 ms^{-1}.~~ This shows that in JADE a considerable fraction of the saltation fluxes was recorded at u* below the perceived threshold friction velocity (about 0.2 ms^{-1}), saltation is more intermit~~tency mainly occurs~~ under weak wind conditions, and becomes non-intermittent for $u_* > 0.3$ ms^{-1}. The ~~increase of~~ $\gamma_b(u_*)$ with decreasing u_* for $u_* < 0.1$ ms^{-1}, is however unexpected. The expected $\gamma_b(u_*)$ for small u_* is as depicted using the dashed line. A likely reason for the unexpected behaviour of $\gamma_b(u_*)$ is that during a wind erosion event, grains in saltation may continue to hop even when u_* is temporarily reduced to small values. The uncertainty in the data also needs to be considered, as the sample size for determining the ratio T_{Q1min}/T_{u*} becomes smaller. More complete datasets are required to answer these questions. ~~If γ_{int} is computed using Q_{1s}, then its maximum reaches about 0.4, similar to that reported in Stout and Zobeck [1997].~~ Finally, γ_c is computed by using Equation (14d) and is found to be around 0.73. For the one-second case, we cannot plot γ_{bint} as a function of u_{*c}, because u_* is not available at such high frequency. We computed γ_c for individual particle size groups (Fig. 6b) using Q_{1sec}, Q_{1min} and Q_{30min}, which is the time fraction of saltation for a given particle size, d, during the saltation event. ~~shows (the maximum of) γ_{int} as function of particle size for the one-second,~~

Formatted ...
Formatted ...
Formatted ...
Formatted ...
Formatted ...
Formatted ...

~~one-minute and 30-minute cases.~~ It is found that ~~In general,~~ $\gamma_a(d)_{int}$ dein~~creases~~ with d_s ~~particle size,~~ i.e., the saltation of larger particles is more intermittent. Also, $\gamma_a(d)_{int}$ inde~~creases~~ with increased averaging time intervals, implying that the small scales features of turbulence play an important role in intermittent saltation.

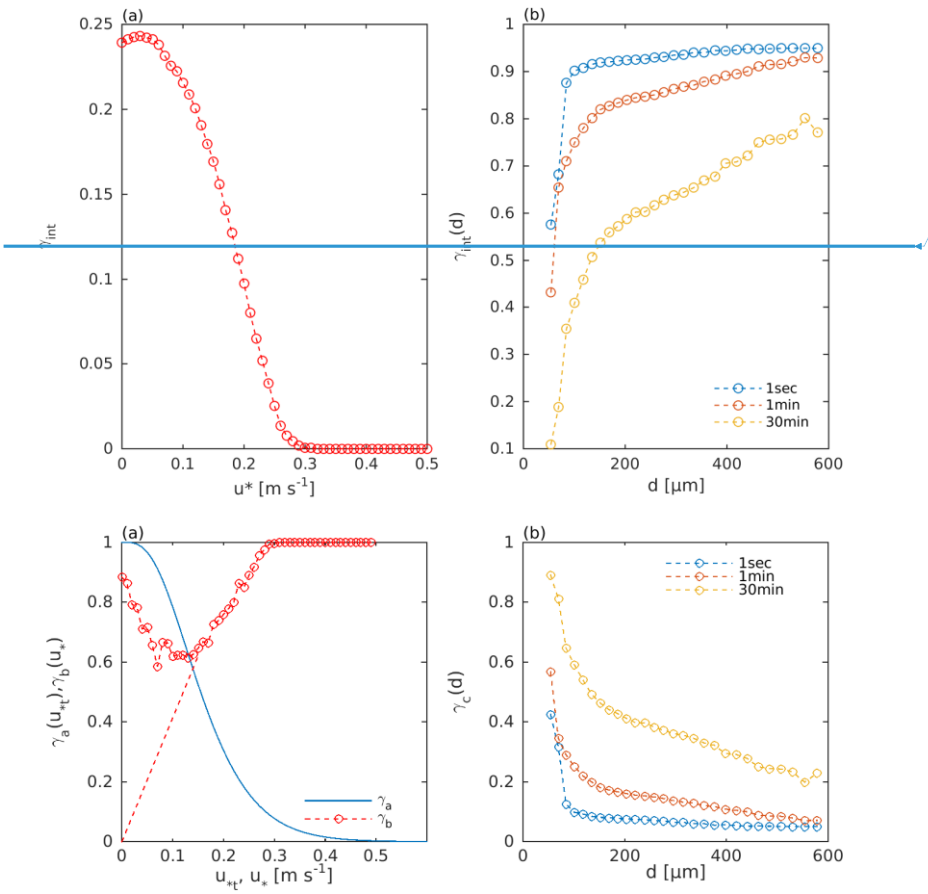

Figure 6: (a) Saltation intermittency function ~~,~~ $\gamma_a(u_{*t})_{int}$, and $\gamma_b(u_*)$. See text for more details.~~computed using Q_{1m} conditionally sampled for $u_* > u_{*t}$;~~ (b) $\gamma_{c\ int}$ as a function of particle size for Q_{1sec}, Q_{1min} and Q_{30min}.
~~the one-second, one-minute and 30-minute cases.~~

3.4 Spectrum of Saltation Fluxes

Spectral analysis is a widely used for characterising the variations of a stochastic process on different scales. Using the JADE data, we computed the power spectrum of saltation fluxes, $P_Q(f)$ at frequency f, and of friction velocity, $P_{u^*}(f)$, using a non-uniform discrete Fourier

Formatted: Not Highlight
Formatted: Not Highlight
Formatted: Not Superscript/ Subscript, Not Highlight
Formatted: Not Highlight
Formatted: Not Highlight
Formatted: Font: Italic, Not Highlight
Formatted: Not Highlight
Formatted: Not Highlight
Formatted: Not Superscript/ Subscript, Not Highlight
Formatted: Not Highlight
Formatted: Justified
Formatted: Not Superscript/ Subscript
Formatted: Not Superscript/ Subscript
Formatted: Font: Not Italic
Formatted: Font: Italic
Formatted: Font: Italic, Subscript
Formatted: Font: Italic
Formatted: Font: Italic, Subscript
Formatted: Font: Italic
Formatted: Font: Italic, Subscript
Formatted: Font: Italic
Formatted: Font: Italic, Subscript
Formatted: Font: Italic
Formatted: Font: Italic
Formatted: Font: Italic
Formatted: Font: Italic, Subscript
Formatted: Font: Italic

transform. For comparison, the power spectra are normalized with the respective variances of the signal. In atmospheric boundary-layer studies, the spectra of various turbulence quantities have been thoroughly investigated (Stull, 1988). Examples for spectra of Reynolds shear stress can be found in McNaughton and Laubach (2000). Fig. 7 shows $P_Q(f)$ and ~~the power spectra of Q and $P_{u*}(f)$~~ (Fig. 7a) as well their co-spectrum (Fig. 7b). $P_Q(f)$ ~~The power spectrum of Q~~ is computed using both Q_{1sec} and Q_{1min}, and $P_{u*}(f)$ ~~that of u_*~~ with u_{*1min}. It is seen that the power spectra of Q and u_* have qualitatively very similar behaviour. Both have a maximum at about 10^{-5} Hz, a minimum at about 10^{-4} Hz and another peak ~~maximum~~ at about $2x10^{-3}$ Hz. The maximum at 10^{-5} Hz is related to the diurnal patterns and changing ~~to~~ synoptic events, which drive the wind erosion episodes, the minimum at 10^{-4} Hz is due to the lack of turbulent winds at the time scale of several hours, while the peak ~~maximum~~ at $2x10^{-3}$ Hz is caused by the minute-scale gusty winds/large eddies in turbulent flows. Also the Q-u_* co-spectrum shows that Q and u_* are most strongly correlated on diurnal/synoptic and gust/large-eddy time scales. $P_Q(f)$ ~~The saltation spectrum~~ computed using Q_{1sec} reveals again the peaks at 10^{-5} Hz and ~~maximum~~ at $2x10^{-3}$ Hz. The ~~However, the~~ power of the Q spectrum then ~~rapidly~~ decreases with frequency. ~~and become relatively weak on time scales smaller than ~ 10 s.~~ As the sampling rate of saltation flux is limited to one second in this study, the features of $P_Q(f)$ at frequencies larger than 0.5 Hz are not resolved.

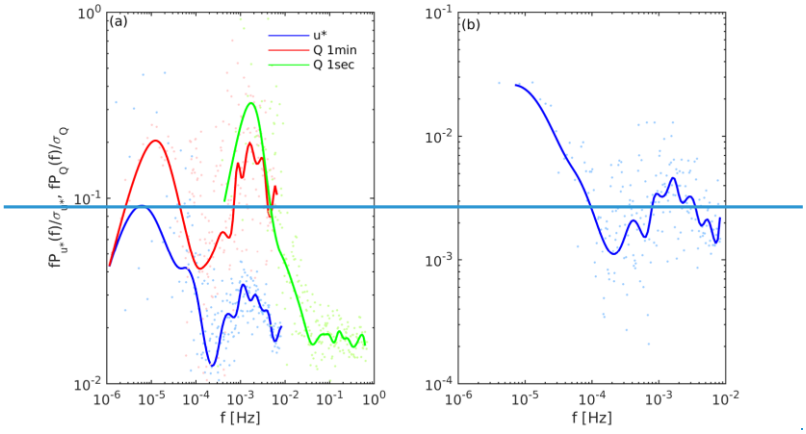

Formatted: Font: Italic
Formatted: Font: Italic, Subscript
Formatted: Font: Italic
Formatted: Font: Italic
Formatted: Subscript
Formatted: Font: Italic
Formatted: Font: Italic
Formatted: Font: Italic, Subscript
Formatted: Font: Italic
Formatted: Font: Italic
Formatted: Font: Italic, Subscript
Formatted: Font: Italic
Formatted: Font: Italic
Formatted: Font: Italic, Subscript
Formatted: Font: Italic
Formatted: Font: Italic
Formatted: Font: Italic, Subscript
Formatted: Font: Not Italic
Formatted: Font: Not Italic

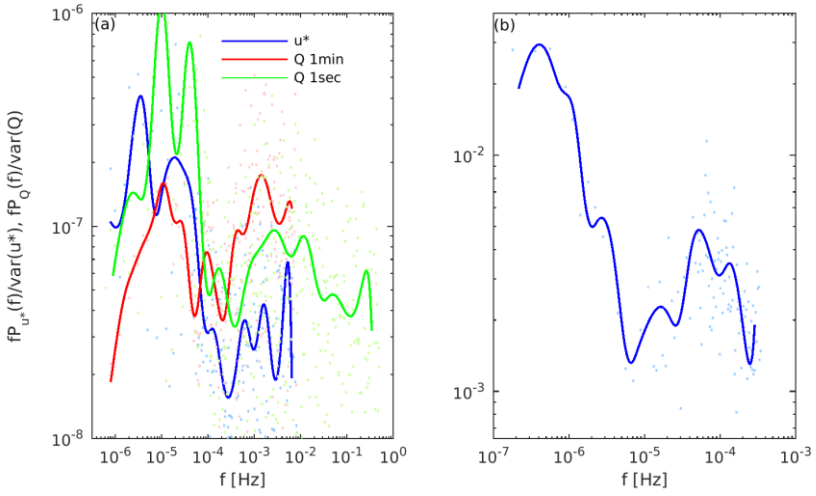

Figure 7: (a) Normalized power spectrum of u_* ~~friction velocity~~ (blue) computed with u_{*1min}, together with the normalized power spectrum of saltation flux computed with Q_{1min} (red) and Q_{1sec} (green). (b) Normalized Q-u_* co-spectrum, computed using with Q_{1min} and u_{*1min}. In both (a) and (b), dots are unsmoothed spectra, and ~~while~~ curves are smoothed spectra.

4. ~~4.2~~ Estimates of Saltation Model Parameters

Given the turbulent nature of saltation, it is rational to treat u_{*t} and c_0 in the saltation model as ~~to be~~ parameters obeying certain probability distributions. To examine the behavior of these parameters, we introduce two coefficients r_{c0} and $r_{u*t,}$ and multiply them respectively by the "theoretical" values of ~~to~~ c_0 and u_{*t} in Equation (2), i.e.,

$$u_{*t} = r_{u*t} u_{*t,theory}$$
$$c_0 = r_{c0} c_{0,theory}$$

As introduced in Section 1, we assumed $c_{0,\,theory} = 2.6$ and computed $u_{*t,\,theory}$ using Equation (1) with observed soil moisture and fraction of cover. The two coefficients r_{c0} and r_{u*t} ~~y~~ are ~~then~~ varied to generate a model estimate of Q using Equations (2) and (3) with observed u_*. The probability distributions of r_{c0} and r_{u*t} are estimated using the following techniques. ~~and the theoretical values of u_{*t} and c_0.~~ Let us ~~We~~ denote the time series of the modelled saltation flux as $Q_{M,i,}$ (i=1,N) and of the corresponding measurement $Q_{D,i}$. The absolute error, δQ_A, and Nash coefficient, I_{Nash}, are used as measures for the goodness of the agreement between the model and the measurement. They are defined as,

$$\delta Q_A = \frac{1}{N}\sum |a_i|$$
$$I_{Nash} = (1 - \sum a_i^2 / \sum b_i^2)$$

with

Formatted: Font: Italic
Formatted: Font: Italic, Subscript
Field Code Changed
Formatted: Font: Italic
Formatted: Font: Italic, Subscript
Formatted: Font: Italic
Formatted: Font: Italic, Subscript
Formatted: English (United States)

$$a_i = Q_{M,i} - Q_{D,i}$$

$$b_i = Q_{M,i} - \frac{1}{N}\sum Q_{M,i}$$

$$c_i = \begin{cases} a_i / Q_{M,i} & Q_{M,i} \neq 0 \\ 0 & \text{else} \end{cases}$$

The prior pdfs of r_{c0} and r_{u*t} are assumed to be uniform. In the numerical experiment, we randomly generate r_{c0} and r_{u*t} and seek their values, such that $\delta Q_A \leq \varepsilon$ and $I_{Nash} > \eta$. These experiments are repeated for Q_{1min} and Q_{30min}. The plots of δQ_A and I_{Nash} as functions of r_{c0} and r_{u*t} show that for certain values of r_{c0} and r_{u*t}, the above conditions are satisfied. Fig. 8 shows that for Q_{1min}, the best simulation is achieved with r_{c0} = 1.23 and r_{u*t} = 1.05, while for the Q_{30min}, with r_{c0} = 0.94 and r_{u*t} = 0.91. This suggest ~~shows~~ that ~~while~~ the "optimal" estimates of u_{*t} and c_0 are close to the corresponding theoretic values, but ~~they~~ are dependent on the time averaging intervals, with both u_{*t} and c_0 being larger for shorter averaging intervals.

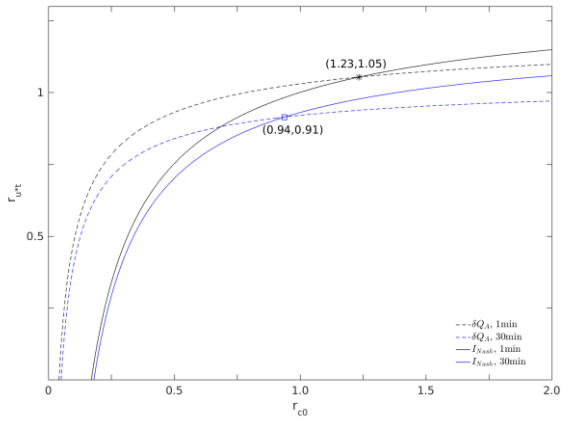

Figure 8: δQ_A and I_{Nash} are both functions of r_{c0} and r_{u*t}. Along the dashed curves, the condition $\delta Q_A = \min$ is satisfied and along the solid curves the condition $I_{Nash} = \max$ is satisfied. The curves are estimated with both Q_{1min} and Q_{30min}. ~~one-minute and 30-minute averaged saltation fluxes.~~

The parameter pdfs $p(r_{u*t})$ and $p(r_{c0})$ are estimated with ~~using~~ the DREAM algorithm, again using the absolute error and the Nash coefficient as goodness of agreement between the model simulated and measured saltation fluxes. The results are shown in Fig. 9. All pdfs are fitted to a Γ-distribution. As seen in Fig. 9a and 9c, the most frequent r_{u*t} values are respectively 1.12 and 1.04 for Q_{1min} and Q_{30min}, close to the estimates of 1.05 and 0.91 found in Fig. 8. For Q_{1min}, r_{u*t} is ~~scatters in the range of~~ ~1.12 ± 0.2 and for Q_{30min} ~~in the range of~~ ~1.04 ± 0.3. This implies that sometimes saltation occurs when u_* is below the theoretical u_{*t} value and sometimes saltation does not occur even when u_* is above it~~the theoretic u_{*t}~~, as already seen in Fig. 6a. In the case of $p(r_{c0})$ (Fig. 9c and 9d), the most frequent values of r_{c0} for Q_{1min} and Q_{30min} are, respectively, 1.04 and 0.92, close to the optimal estimates of 1.23 and 0.94 shown ~~found~~ in Fig.

Formatted: Font: Italic

Formatted: Font: Italic, Subscript

Formatted: Font: Italic

Formatted: Font: Italic, Subscript

8. But ~~But~~ r_{c0} varies ~~scatters~~ over a wide range, for instance, for Q_{30min} between 0.5 and 5, i.e., c_0 is a rather stochastic parameter.

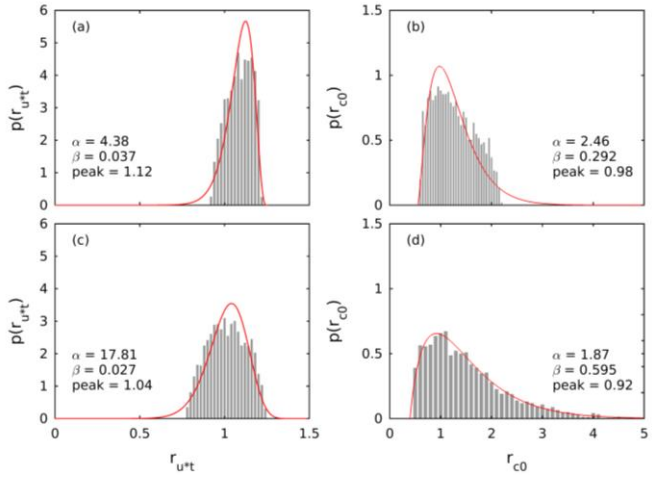

Figure 9: (a) Parameter pdf $p(r_{u*t})$ for 1-min averaged saltation fluxes; (b) as (a), but for $p(r_{c0})$; (c) and (d), as (a) and (b), but for 30-min averaged saltation fluxes.

In nature, many factors influence sediment transport, but the stochasticity of the parameters is determined primarily by the turbulent fluctuations of friction velocity (or ~~representing~~ surface shear stress), the randomness of threshold friction velocity, and soil particle size distribution (representing particle response to forcing). Studies have shown, for instance, that small changes in soil moisture can have large influences on saltation [Ishizuka et al. 2008] and soil moisture in the very top soil layer can vary significantly over relatively short time periods. Over the period of 18 days during JADE ~~this study is based on~~ soil moisture in the top 0.05 m layer varied between 0.02 and 0.04 m^3m^{-3} (4 and 8% in relative soil moisture, assuming a saturation soil moisture of 0.5 m^3 m^{-3}). In this study, the influence of soil moisture on saltation is accounted for via Equation (1) using the soil moisture measurements in the top 0.05m layer (see also Fig. 4a in Shao et al. 2011). While measured soil moisture is used in the wind erosion model, the randomness associated with its spatial-temporal variations is not, which is ~~The uncertainty in the wind erosion parameters arising from soil moisture is~~ most likely reflected in the stochasticity of u_{*t}.

The stochasticity of c_0 arises because saltation fluctuates, depending on ~~is more likely related to~~ turbulence and particle size. To demonstrate ~~show~~ this, we divided the time series of the saltation fluxes into two subsets, one with $Q_{D,i} \leq 3$ g $m^{-1}s^{-1}$ representing weak saltation and one with $Q_{D,i} > 3$ g $m^{-1}s^{-1}$ representing significant saltation. This separation is arbitrary but sufficient for making the point that c_0 ~~wind erosion parameters~~ depends on u_* ~~which is~~, also a measure of turbulence intensity. The parameter pdfs, $p(r_{u*t})$ and $p(r_{c0})$, for the subset $Q_{D,i} \leq 3$ g $m^{-1}s^{-1}$ is shown in Fig. 10. For ~~Q_{1m}~~ Q_{1min} and Q_{30min}, the most frequent r_{u*t} values are now respectively 0.99 and 0.85, somewhat smaller than the estimated values for the full set (~~see~~ Fig. 9). In comparison, the most frequent r_{c0} values are now respectively 0.30 and 0.29, three to four times ~~much~~ smaller than for the case when the full set is considered (~~see~~ Fig. 9). This suggests that c_0 has a clear dependency on u_* and is smaller for smaller u_*. This is because ~~when~~ saltation is more intermittent in the case of smaller u_* (i.e. smaller excess shear stress)~~,~~ and thus, c_0, a

Formatted: Superscript
Formatted: Superscript
Formatted: Superscript
Formatted: Superscript
Formatted: English (United States)
Formatted: Font: Italic
Formatted: Font: Italic, Subscript
Formatted: Font: Italic
Formatted: Font: Italic, Subscript
Formatted: Font: Italic
Formatted: Font: Italic, Subscript

descriptor of the relation between time-averaged saltation flux and friction velocity, is smaller for more intermittent saltation. ~~as also seen in Fig. 6a.~~

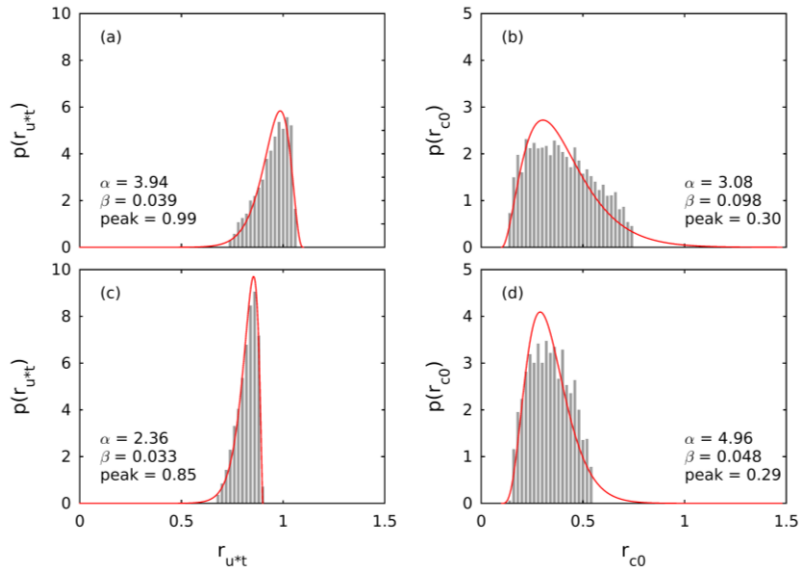

Figure 10: As Fig. 9, but estimated using the time series of saltation fluxes which satisfy $Q_{D,i} \leq 3$ g m^{-1} s^{-1}.

We fit~~ted~~ the pdfs, $p(r_{u*t})$ and $p(r_{c0})$, for individual particle size bins and ~~. It is~~ found that the most frequent r_{u*t} values do not differ substantially among the particle sizes, but r_{c0} depends systematically on particle size. For example, the most frequent r_{c0} values for 101, ~~0.7,~~ 151~~.2~~, 203, ~~.3,~~ 3154~~.5~~ and 3987~~.7~~ µm are, respectively, 0.548, 1.3~~1~~, 1.765, 3.106 ~~and 4.00~~. These values are obtained by first estimating $p(r_{c0})$ for the individual particle size bins with the measured saltation flux for the corresponding bins and then normalizing $p(r_{c0})$ with the mass fraction of the size bins of the parent soil. A least squares curve fitting shows that the most frequent r_{c0} value depends almost perfectly (R^2 = 0.996) linearly on particle size:

$$r_{c_0} = 0.012d - 0.59 \qquad (156)$$

for the particle size range (100 to 400 µm) we tested, with d being particle size in µm.

We have shown that both u_{*t} and c_0 satisfy certain pdfs that ~~which~~ depend on the properties of the surface, atmospheric turbulence and soil particle size. Fig. 9 shows that for a fixed choice of u_{*t} and c_0, even if they are "optimally" chosen, a portion of the measurements cannot be represented by the model. Then, how does the saltation model perform if a single fixed u_{*t} and a single fixed c_0 are used as is often the case in aeolian models? The $p(Q)$ computed using the model and derived from the JADE measurements are shown for Q_{1min} and Q_{30min} in Fig. 11. ~~In this case,~~ T~~t~~he ~~saltation~~ model is applied to estimate the saltation flux for ~~the~~ individual particle size groups using the optimally estimated u_{*t} and c_0 (with r_{u*t} = 1.12 and r_{c0} = 1.04 for Q_{1min}, and r_{u*t} = 1.04 and r_{c0} = 0.92 for Q_{30min}) and the total ~~(particle-size-integrated)~~ saltation flux is computed by integration over all particle size groups, i.e., using Equation (3). ~~using the u_{*t} and~~

Formatted: Font: Italic
Formatted: Superscript
Formatted: Font: Italic
Formatted: Font: Italic, Subscript
Formatted: Font: Italic
Formatted: Font: Italic, Subscript
Formatted: Font: Italic
Formatted: Font: Italic, Subscript

~~c_0 optimally estimated.~~ Fig. 11 shows that for this option, the model over predicts ~~and~~ the probability of large Q, but under predicts the probability of small Q, in both cases of Q_{1min} and Q_{30min}. Obviously, to better reproduce the Q_{1min} *and* Q_{30min} pdfs, more values of r_{u^*t} and r_{c0} sampled from the parameter pdfs are required. We have therefore modelled Q_{1min} with other choices of r_{u^*t} (1.12 and 0.56) and r_{c0} (2.08, 0.01) and plotted the corresponding Q_{1min} pdfs as well as the averaged Q_{1min} pdf of the three simulations. Similarly, we performed Q_{30min} model simulations with other r_{u^*t} (1.04) and r_{c0} (1.84) values and examined the Q_{30min} pdfs. With the additional choices of the r_{u^*t} and r_{c0} values, the Q_{1min} and Q_{30min} pdfs can be better reproduced.

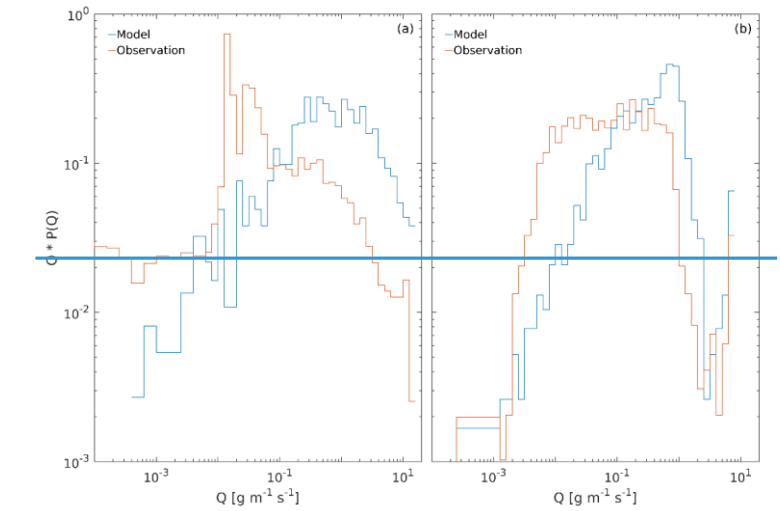

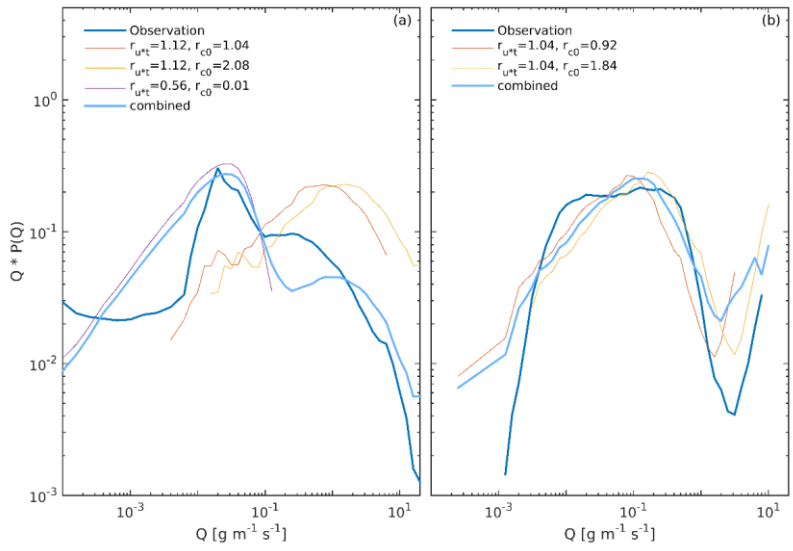

Formatted: Font: Italic
Formatted: Subscript
Formatted: Subscript
Formatted: Font: Italic
Formatted: Font: Italic, Subscript
Formatted: Font: Italic
Formatted: Font: Italic, Subscript
Formatted: Font: Italic
Formatted: Font: Italic
Formatted: Font: Italic, Subscript
Formatted: Font: Italic
Formatted: Font: Italic, Subscript
Formatted: Font: Italic
Formatted: Font: Italic, English (United States), Subscript
Formatted: Font: Italic
Formatted: Font: Italic, Subscript
Formatted: Font: Italic
Formatted: Font: Italic, Subscript
Formatted: Font: Italic
Formatted: Font: Italic, Subscript
Formatted: English (United States)
Formatted: English (United States), Subscript
Formatted: Font: Not Italic
Formatted: Font: Not Italic, English (United States)
Formatted: Font: Not Italic
Formatted: English (United States)
Formatted: English (United States), Subscript
Formatted: Subscript
Formatted: Font: Not Italic
Formatted: Font: Italic
Formatted: Font: Italic, Subscript
Formatted: Font: Not Italic
Formatted: Font: Italic
Formatted: Font: Italic, Subscript
Formatted: Subscript
Formatted: Font: Italic
Formatted: Font: Italic, Subscript
Formatted: Font: Italic
Formatted: Font: Italic, Subscript
Formatted: Font: Italic
Formatted: Font: Italic, Subscript
Field Code Changed

Figure 11: (a) Probability density functions of observed Q and simulated Q for 1-min averages with several choices of $r_{u^*_t}$ and r_{c0}; (b) as (a), but for 30-min averages.

5. 5. Summary

In this paper, we have used the JADE data of saltation fluxes (resolution one second) and frictional velocity (resolution one minute) to analyze the statistical behavior of turbulent saltation and estimate the probability distribution of two of the most important parameters in a saltation model, namely, the threshold friction velocity, u_{*t}, and saltation coefficient, $c_{0.}$, in a saltation model.

Saltation fluxes show a rich variations on different scales. It is found that while the widely used $Q \sim u_*^3$ relationship holds in general, it can vary significantly between different wind erosion events. In several wind erosion events observed in JADE, saltation hysteresis occurred. We examined the probability density function of the saltation fluxes, $p(Q)$, and found that it generally behaves like $Q^{-\alpha}$. with $\alpha \sim 1$. For $Q_{1s_{ec}}$, there is a distinct change in α at $Q = 3 \sim 4$ g m^{-1} s^{-1} with $\alpha \sim = 10.8 \sim 0.9$ for smaller Q and $\alpha \sim = 4.0$ larger Q. It is shown that $p(Q)$ is dependent on the averaging time intervals as a consequence of saltation intermittency.

We introduced the saltation intermittency functions $\gamma_a(u_{*t})$, $\gamma_b(u_*)$ and redefined saltation intermittency γ_c defined saltation intermittency, γ_{int}, as the fraction of time during which saltation occurs at a given point in a given time period, and computed these saltation intermittency measures γ_{int} using the JADE saltation flux measurements. It is found that $\gamma_a(u_{*t})$ is one at $u_{*t} = 0$ and decreases to zero at about $u_{*t} = 0.5$ ms^{-1}. For $u_{*t} = 0.2$ ms^{-1}, γ_a is 0.35. For Q_{1min}, , $\gamma_b(u_*)$ increases from about 0.6 at $u_* \sim 0.1$ ms^{-1} to about one at $u_* = 0.3$ ms^{-1}. This shows that a considerable fraction of the saltation fluxes occurs at small friction velocity and saltation is more intermittent under weak wind conditions and is almost non-intermittent for $u_* > 0.3$ m s^{-1}. It is found that $\gamma_b(u_*)$ increased with decreasing u_* for $u_* < 0.1$ ms^{-1} which is unexpected. Overall, γ_c is found to be around 0.73. We computed γ_c as function of particle size and found that $\gamma_c(d)$ decreases with d, i.e., the saltation of larger particles is more intermittent. Also, $\gamma_c(d)$ increases with increased averaging time intervals, implying that the small scales features of turbulence play an important role in intermittent saltation. For Q_{1m} conditionally sampled with $u_* > u_{*c}$, it is found that γ_{int} has a maximum of about 0.25 for small u_{*c} and decreases to zero at about $u_{*c} = 0.3$ ms^{-1}. This shows that saltation intermittency mainly occurs under weak wind conditions. The γ_{int} computed using Q_{1s} has a maximum of about 0.4. We have also computed γ_{int} as a function of different particle sizes and found that γ_{int} in general increases with particle size.

The power spectra of Q saltation flux and u_* friction velocity are found to have qualitatively similar behaviour. Both have a maximum at about 10^{-5} Hz, a minimum at about 10^{-4} Hz and another peak maximum at about 2×10^{-3} Hz. The maximum at 10^{-5} Hz is related to the diurnal to synoptic events that which drive wind erosion episodes, the minimum at 10^{-4} Hz is due to the lack of turbulent wind fluctuations at the time scale of several hours, while the peak maximum at 2×10^{-3} Hz is caused by the minute-scale gustsy winds/large eddies in turbulent flows. The power of the saltation rapidly decreases with frequency and becomes relatively weak at frequencies of 0.1 Hz.

The posterior pdfs of the two parameters weare estimated using the DREAM algorithm applied to the JADE saltation flux measurements. While both u_{*t} and c_0 have clear physical interpretations, they are both stochastic parameters satisfying certain parameter pdfs. They also

Formatted: Font: Italic
Formatted: Font: Italic, Subscript
Formatted: Subscript
Formatted: Font: Italic
Formatted: Font: Italic, Subscript
Formatted: Font: Italic
Formatted: Font: Italic, Subscript
Formatted: Font: Italic
Formatted: Font: Italic, Subscript
Formatted: Font: Italic
Formatted: Font: Italic, Subscript
Formatted: Font: Italic
Formatted: Font: Italic, Subscript
Formatted: Font: Italic
Formatted: Font: Italic, Subscript
Formatted: Not Highlight
Formatted: Font: Italic
Formatted: Font: Italic
Formatted: Font: Italic, Subscript

~~appear to be~~ dependent on the intervals of time averaging. Both u_{*t} and c_0 for Q_{1min} ~~the 1-min averages~~ are larger than for ~~the~~ Q_{30min} ~~30-min averages~~. The pdf of u_{*t} shows that it has a most frequent value close to the theoretical value, but can vary over ~~in~~ a range of 20% to 30%. ~~Therefore, the use of the most frequent value of u_{*t} in the saltation model seems to be reasonable. In contrast, the pdf~~ The pdf of c_0 shows ~~that it~~ scatter~~s~~ over a ~~much~~ wide~~r~~ range and it is ~~. This suggests that it is rather~~ unlikely that a universal c_0 exists. In a saltation model, even if the optimally estimated ~~and the use of the most frequent value of~~ c_0 is used, considerable ~~would not reduce the~~ scatter between the model and the data would remain. The likely reason for the stochasticity in u_{*t} may be the temporal and spatial variations of particle cohesion, surface roughness, particle shape etc. which cannot be well represented by a fixed deterministic value, and the relatively large uncertainty in c_0 may be that this ~~it is~~ parameter depends ~~ing~~ on additional factors (e.g. u_* ~~friction velocity~~ and soil particle size distribution) and is related to the fluctuations and intermittency of saltation. It may also be that saltation in reality is never in equilibrium as Bagnold (1941), Kawamura (1964) and Owen (1964) conceptualized, because due to turbulen~~ce~~ce~~t fluctuations~~, sand grains are continuously entrained at different rates into the airflow and a continuous flow- and particle-motion feedback takes place. As a consequence, it is difficult to treat c_0 as a universal constant.

In this study, we highlighted the need to better understand saltation as a turbulent process and the stochasticity of saltation model parameters. The concept of threshold friction velocity as a stochastic variable was put forward in Shao (2001). Raffaele et al. (2016) examined the pdf of u_{*t} using data compiled from publications. Raffaele et al. (2018) studied how u_{*t} uncertainties propagate in saltation flux calculations and reported that in the case of small excess shear stress, all models they tested amplify the uncertainty in estimated saltation flux, especially for coarse sand. This finding is consistent with our notion that c_0 also is a stochastic variable. Due to the stochasticity of the model parameters, the saltation model cannot reproduce the observation even with the optimally estimated parameters (e.g. under estimation of weak saltation fluxes and over estimation of strong saltation fluxes). A combination of several pairs of model parameters appears to be required to reasonably reproduce the pdfs of saltation fluxes.

Our estimates of the parameter uncertainties is based on the data of a relatively simple aeolian surface. For more complex surfaces, we expect the parameter uncertainties to be even more pronounced.

Acknowledgement: This research is funded by the National Natural Science Foundation of China (~~Control mechanism of groundwater-soil-vegetation continuum on dust emission in desert playas, No. 41571090~~No. 41571090, 41201539). The data used in this study we~~a~~re obtained in JADE (the Japan Australian Dust Experiment) by M. Ishizuka, M. Mikami, J. F. Leys, Y. Yamada, and S. Heidenreich. We are grateful to P. Schlüter and Q. Xia for support with data processing. We also wish to thank Dr. J. Gillies, Dr. M. Klose and an anomalous referee for their very helpful comments which prompt us to rework on a number of issues presented in the first version of the paper.

References:

Anderson, R. S. and P. K. Haff (1988): Simulation of Eolian Saltation. Science 241, 820-823. DOI: 10.1126/science.241.4867.820

Formatted: Font: Italic
Formatted: Font: Italic, Subscript
Formatted: Font: Italic
Formatted: Font: Italic, Subscript
Formatted: Font: Italic
Formatted: Font: Italic, Subscript
Formatted: Font: Italic
Formatted: Font: Italic, Subscript
Formatted: Font: Italic
Formatted: Font: Italic, Subscript
Formatted: Font: Italic
Formatted: Font: Italic, Subscript
Formatted: Font: Italic
Formatted: Font: Italic, Subscript
Formatted: Font: Times New Roman, Not Bold, Font color: Auto
Formatted: Indent: Left: 0 cm, Hanging: 0,02 cm, Space After: 11,25 pt
Formatted: Font: Times New Roman, Not Bold, Font color: Auto
Formatted: Font: Times New Roman, Not Bold
Formatted: Font: Not Italic, Font color: Auto
Formatted: Font color: Auto

Bagnold, R.A. (1941): The Physics of Blown Sand and Desert Dunes. Methuen, London, 265pp.

Butterfield, G. R. (1991): Grain transport rates in steady and unsteady turbulent airflows. Acta Mechanica, Suppl. 1, 97-122.

Davidson-Arnott, R. G. D., and B. O. Bauer (2009): Aeolian sediment transport on a beach: Thresholds, intermittency, and high frequency variability. Geomorphology 105: 117–126.

Dupont, S., G. Bergametti, B. Marticorena, and S. Simoëns (2013), Modeling saltation intermittency, J. Geophys. Res. Atmos., 118, 7109–7128, doi:10.1002/jgrd.50528.

Ellis, J. T., D. Sherman, E. J. Farrell and B. L. Li (2012): Temporal and spatial variability of aeolian sand transport: Implications for field measurements. Aeolian Research 3(4):379-387. DOI: 10.1016/j.aeolia.2011.06.001.

Fecan, F., Marticorena B., Bergametti G. (1999) Parametrization of the increase of the aeolian erosion threshold wind friction velocity due to soil moisture for arid and semi-arid areas. Annales Geophysicae 17:149–157

Gillette, D.A., E. Hardebeck and J. Parker (1997) Large-scale variability of wind erosion mass flux rates at Owens Lake 2. Role of roughness change, particle limitation, change of threshold friction velocity, and the Owen effect. J. Geophys. Res. 102, 25,989-25,998

Ishizuka, M., Mikami, M., Leys, J. F., Yamada, Y., Heidenreich, S., Shao, Y., McTainsh, G. H. (2008): Effects of soil moisture and dried raindroplet crust on saltation and dust emission. J. Geophys. Res. 113, D24212, doi:10.1029/2008JD009955

Ishizuka, M., Mikami, M., Leys, J. F., Shao, Y., Yamada, Y. and Heidenreich, S. (2014): Power law relation between size-resolved vertical dust flux and friction velocity measured in a fallow wheat field. Aeolian Research 12:87-99. DOI: 10.1016/j.aeolia.2013.11.002

Klose, M., Y. Shao, X. Li, H. Zhang, M. Ishizuka, M. Mikami, and J. F. Leys (2014): Further development of a parameterization for convective turbulent dust emission and evaluation based on field observations. J. Geophys. Res. Atmos. 119, 10,441–10,457, doi:10.1002/2014JD021688.

Kok, J.F., N.M. Mahowald, G. Fratini, J.A. Gillies, M. Ishizuka, J.F. Leys, M. Mikami, M.S. Park, S.U. Park, R.S. Van Pelt, T.M. Zobeck (2014): An improved dust emission model – Part 1: model description and comparison against measurements. Atmos. Chem. Phys. 14, 13023–13041

Kawamura, R. (1964): Study of sand movement by wind. In: Hydraulic Eng. Lab. Tech. Rep., University of California, Berkeley, HEL-2-8, pp 99–108

Leys, J. F. (1998): Wind erosion processes and sediments in southeastern Australia. Ph.D. Thesis, Griffith University, Brisbane

Namikas, S. L., B. O. Bauer and D. Sherman (2003): Influence of averaging on shear velocity estimates for aeolian transport modeling. Geomorphology 53, 235-246, DOI: 10.1016/S0169-555X(02)00314-8

Formatted: Font color: Auto

Field Code Changed

Formatted: Font color: Auto

McKenna-Neuman, C., N. Lancaster, and W. G. Nickling (2000): The effect of unsteady winds on sediment transport on the stoss slope of a transverse dune, Silver Peak, NV, USA. Sedimentology 47: 211–226

McNaughton, K. G. and J. Laubach (2000): Power Spectra and Cospectra for Wind and For Wind and Scalars in a Disturbed Surface Layer at the Base of an Advective Inversion. Boundary-Layer Meteorology 96: 143–185.

Owen, R. P. (1964): Saltation of uniform grains in air. J. Fluid. Mech. 20, 225–242.

Raffaele, L., L. Bruno, F. Pellerey and L. Preziosi, 2016: Windblown sand saltation: A statistical approach to fluid threshold shear velocity. Aeolian Research 23, 79–91, http://dx.doi.org/10.1016/j.aeolia.2016.10.002

Raffaele, L., L. Bruno and G.F.S. Wiggs, 2018: Uncertainty propagation in aeolian processes: From threshold shear velocity to sand transport rate. Geomorphology, https://doi.org/10.1016/j.geomorph.2017.10.028

Raupach, M.R., Gillette D.A. and Leys J.F. (1993): The effect of roughness elements on wind erosion thresholds. J. Geophys. Res. 98:3023–3029.

Sadegh, M. and J. A. Vrugt (2014): Approximate Bayesian computation using Markov Chain Monte Carlo simulation: DEARM$_{(ABC)}$. Water Resour. Res. 50, doi:10.1002/2014WR015386

Shao, Y. and Lu H. (2000): A simple expression for wind erosion threshold friction velocity. J. Geophys. Res. 105:22,437–22,443

Shao, Y. (2001): Physics and Modelling of Wind Erosion. 1st Edition, Kluwer Academic Publishers.

Shao, Y., M. Ishizuka, M. Mikami, and J. F. Leys (2011): Parameterization of size-resolved dust emission and validation with measurements. J. Geophys. Res., 116, D08203, doi:10.1029/2010JD014527

Shao, Y. and Mikami, M. (2005): Heterogeneous Saltation: Theory, Observation and Comparison. Boundary-Layer Meteorol. 115:359. doi:10.1007/s10546-004-7089-2

Sherman, D., B. L. Li, J. T. Ellis and C. Swann (2017): Intermittent aeolian saltation: A protocol for quantification. Geographical Review 1–19. DOI: 10.1111/gere.12249.

Storn, R. and Price, K. (1997): Differential Evolution – a simple and efficient heuristic for global optimization over continuous spaces. J. Global Optim. 11, 341-359

Stout, J. E. and T. M. Zobeck (1997): Intermittent saltation. Sedimentology 44, 959-970

Stull, R. B. (1988): An Introduction to Boundary Layer Meteorology. Kluwer Academic Publishers.

Formatted: Font: 12 pt
Formatted: Font: 12 pt, Not Bold, English (United States)
Formatted: Snap to grid
Formatted: Font: 12 pt, Not Bold
Formatted: Font: 12 pt, Not Bold, English (United States)
Formatted: Font: 12 pt, Not Bold
Formatted: Font: 12 pt, Not Bold
Formatted: Font: 12 pt, Not Bold, English (United States)
Formatted: Font: 12 pt, Not Italic, English (United States)
Formatted: Font: 12 pt, English (United States)
Formatted: Font: 12 pt, Not Bold, English (United States)
Formatted: Font: 12 pt, English (United States)
Formatted: Font: 12 pt
Formatted: Font color: Auto
Formatted: Font: (Default) Times New Roman, 12 pt
Formatted: Justified
Formatted: Font: (Default) Times New Roman, 12 pt
Formatted: Font: (Default) Times New Roman, 12 pt
Formatted: Font: (Default) Times New Roman, 12 pt
Formatted: Font: (Default) Times New Roman, 12 pt
Formatted: Font: (Default) Times New Roman, 12 pt
Formatted: Font: (Default) Times New Roman, 12 pt
Formatted: Font: (Default) Times New Roman, 12 pt, English (United States)
Formatted: Font: (Default) Times New Roman, 12 pt
Formatted: Font: (Default) Times New Roman, 12 pt, English (United States)
Formatted: Snap to grid
Formatted: Superscript
Formatted: Font color: Auto
Formatted: English (United States)
Formatted: Font: (Default) Times New Roman, 12 pt, English (United States)
Formatted: Font: (Default) Times New Roman, 12 pt
Formatted: Font: (Default) Times New Roman, 12 pt
Formatted: Justified
Formatted: English (United Kingdom)

Vrugt, J. A., ter Braak, C. J. F., Diks, G. H., Robinson, B. A., and Hyman, J. M. (2011): Accelerating Markov Chain Monte Carlo Simulation by Differential Evolution with Self-Adaptive Randomized Subspace Sampling. Int. J. Nonlin. Sci. Num. 10(3), 273-290. doi:10.1515/IJNSNS.2009.10.3.273

Vrugt, J. A. and M. Sadegh (2013): Toward diagnostic model calibration and evaluation: Approximate Bayesian computation. Water Resour. Res. 49, 4335-4345. doi:10.1002/wrcr.20354

White, B.R. (1979): Soil transport by winds on Mars. J. Geophys. Res. 84, 4643-4651

Yamada Y., Mikami M., Nagashima H. (2002): Dust particle measuring system for streamwise dust flux. J. Arid Land Studies 11(4): 229–234